

1       **Rain or Snow: Hydrologic Processes, Observations,**  
2                   **Prediction, and Research Needs**

3  
4   Adrian A. Harpold\*, University of Nevada, Reno, aharpold@cabnr.unr.edu

5   Michael Kaplan, Desert Research Institute, michael.kaplan@dri.edu

6   P. Zion Klos, University of Idaho, zion.klos@gmail.com

7   Timothy Link, University of Idaho, tlink@uidaho.edu

8   James P. McNamara, Boise State University, jmcnamar@boisestate.edu

9   Seshadri Rajagopal, Desert Research Institute, Seshadri.Rajagopal@dri.edu

10   Rina Schumer, Desert Research Institute, rina@dri.edu

11   Caitriana M. Steele, New Mexico State University, caiti@nmsu.edu

12  
13  
14   \*Corresponding author

17 **Abstract**

18 The phase of precipitation when it reaches the Earth surface is a first-order driver of hydrologic  
19 processes in a watershed. The presence of snow, rain, or mixed phase precipitation affect the  
20 initial and boundary conditions that drive hydrological models. Despite their foundational  
21 importance to terrestrial hydrology, typical phase prediction methods (PPM) specify phase based  
22 on near-surface air temperature only. Our review conveys the diversity of tools available for  
23 PPM in hydrological modeling and the advancements needed to improve predictions in complex  
24 terrain with large spatiotemporal variations in precipitation phase. Initially, we review the  
25 processes and physics that control precipitation phase as relevant to hydrologists, focusing on the  
26 importance of processes occurring aloft. There are a wide range of options for field observations  
27 of precipitation phase, but a lack of a robust observation networks in complex terrain. New  
28 remote sensing observations have potential to increase PPM fidelity, but generally require  
29 assumptions typical of other PPM and field validation before they are operational. We review  
30 common PPM and find that accuracy is generally increased at finer measurement intervals and  
31 by including humidity information. One important tool for PPM development is atmospheric  
32 modeling, which include microphysical schemes that have not been effectively linked to  
33 hydrological models or validated against near-surface precipitation phase observations. The  
34 review concludes by describing key research gaps and recommendations to improve PPM,  
35 including better incorporation of atmospheric information, improved validation datasets, and  
36 regional-scale gridded data products. Two key points emerge from this synthesis for the  
37 hydrologic community: 1) current PPM algorithms are too simple and are not well-validated for  
38 most locations, 2) lack of sophisticated PPM increases the uncertainty in estimation of  
39 hydrological sensitivity to changes in precipitation phase at local to regional scales. PPM are a  
40 critical research frontier in hydrology that requires scientific cooperation between hydrological  
41 and atmospheric modelers and field hydrologists.

42

43 **Keywords:** precipitation phase, snow, rain, hydrological modeling

44

45 1. Introduction and Motivation

46 As climate warms, a major hydrologic shift in precipitation phase from snow to rain is expected  
47 to occur across temperate regions that are reliant on mountain snowpack for water resources  
48 (Bales et al., 2006; Barnett et al., 2005). Continued changes in precipitation phase are expected

49 to alter snowpack dynamics and streamflow timing and amounts (Cayan et al., 2001; Fritze et al.,  
50 2011; Luce and Holden, 2009; Klos et al., 2014; Berghuijs et al., 2014; Jepsen et al., 2016),  
51 increase rain-on snow flooding (McCabe et al., 2007), and challenge our ability to make accurate  
52 water supply forecasts (Milly et al., 2008). Accurate estimations of precipitation inputs are  
53 required for effective hydrological modeling in both applied and research settings. Snow storage  
54 delays the transfer of precipitation into surface runoff and subsurface infiltration (Figure 1),  
55 affecting the timing and magnitude of peak flows (Wang et al., 2016), hydrograph recession  
56 (Yarnell et al., 2010) and the magnitude and duration of summer baseflow (Safeeq et al., 2014;  
57 Godsey et al., 2014). Moreover, the altered timing and rate of snow versus rain inputs can  
58 modify the partitioning of water to evapotranspiration versus runoff (Wang et al., 2013).  
59 Misrepresentation of precipitation phase within hydrologic models thus propagates into spring  
60 snowmelt dynamics (Harder and Pomeroy, 2013; Mizukami et al., 2013; White et al., 2002; Wen  
61 et al., 2013) and streamflow estimates used in water resource forecasting (Figure 1). The  
62 persistence of streamflow error is particularly problematic for hydrological models that are  
63 calibrated on observed streamflow because this error can be compensated for by altering  
64 parameters that control other states and fluxes in the model (Minder, 2010; Shamir and  
65 Georgakakos, 2006; Kirchner, 2006). Expected changes in precipitation phase from climate  
66 warming presents a new set of challenges for effective hydrological modeling (Figure 1). A  
67 simple yet essential issue for nearly all runoff generation questions is this: Is precipitation falling  
68 as rain, snow, or a mix of both phases?

69

70 Despite advances in terrestrial process-representation within hydrological models in the past  
71 several decades (Fatichi et al., 2016), most state-of-the-art models rely on simple empirical  
72 algorithms to predict precipitation phase. For example, nearly all operational models used by the  
73 National Weather Service River Forecast Centers in the United States use some type of  
74 temperature-based precipitation phase partitioning methods (PPM) (Pagano et al., 2014). These  
75 are often single or double temperature threshold models that do not consider other conditions  
76 important to the hydrometeor's energy balance. Although forcing datasets for hydrological  
77 models are rapidly being developed for a suite of meteorological variables, to date no gridded  
78 precipitation phase product has been developed over a regional to global scale. Widespread  
79 advances in both simulation of terrestrial hydrological processes and computational capabilities

80 may have limited improvements on water resources forecasts without commensurate advances in  
81 PPM.

82

83 Recent advances in PPM incorporate effects of humidity (Harder and Pomeroy, 2013; Marks et  
84 al., 2013), atmospheric temperature profiles (Froidurot et al., 2014), and remote sensing of phase  
85 in the atmosphere (Minder, 2010; Lundquist et al., 2008). A challenge to improving and selecting  
86 PPM is the lack of validation data. In particular, reliable ground-based observations of phase are  
87 sparse, collected at the point scale over limited areas, and are typically limited to research rather  
88 than operational applications (Marks et al., 2013). The lack of observations is particularly  
89 problematic in mountain regions where snow-rain transitions are widespread and critical for  
90 regional water resource evaluations (Klos et al., 2014). For example, direct visual observations  
91 have been widely used (Froidurot et al., 2014; Knowles et al., 2006; U.S. Army Corps of  
92 Engineers, 1956), but are decreasing in number in favor of automated measurement systems.  
93 Automated systems use indirect methods to accurately estimate precipitation phase from  
94 hydrometeor characteristics (i.e. disdrometers), as well as coupled measurements that infer  
95 precipitation phase based on multiple lines of evidence (e.g. co-located snow depth and  
96 precipitation). Remote sensing is another indirect method that typically uses radar returns from  
97 the ground and space-borne platforms to infer hydrometeor temperature and phase. A  
98 comprehensive description of the advantages and disadvantages of current measurement  
99 strategies, and their correspondence with conventional PPM, is needed to determine critical  
100 knowledge gaps and research opportunities.

101

102 New efforts are needed to advance PPM to better inform hydrological models by integrating new  
103 observations, expanding the current observation networks, and testing techniques over regional  
104 variations in hydroclimatology. While calls to integrate atmospheric information are an  
105 important avenue for advancement (Feiccabrino et al., 2013), hydrological models ultimately  
106 require accurate and validated phase determination at the land surface. Moreover, any  
107 advancement that relies on integrating new information or developing a new PPM technique will  
108 require validation and training using ground-based observations. To make tangible advancements  
109 in hydrological modeling, new techniques and datasets must be integrated with current modeling  
110 tools. The first step towards improved hydrological modeling in areas with mixed precipitation

111 phase is educating the scientific community about current techniques and limitations that convey  
112 towards gaps where research is needed.

113

114 Our review paper is motivated by a lack of a comprehensive description of the state-of-the-art  
115 PPM and observation tools. Therefore, we describe the current state of the science in a way that  
116 clarifies the correspondence between techniques and observations and highlights current  
117 strengths and weaknesses in the science. Specifically, subsequent sections will review: 1) the  
118 processes and physics that control precipitation phase as relevant to field hydrologists, 2) current  
119 options available for observing precipitation phase and related measurements common in remote  
120 field settings, 3) existing methods for predicting and modeling precipitation phase, and 4)  
121 research gaps that exist regarding precipitation phase estimation. The overall objective is to  
122 convey a clear understanding of the diversity of tools available for PPM in hydrological  
123 modeling and the advancements needed to improve predictions in complex terrain characterized  
124 by large spatiotemporal variations in precipitation phase.

125

## 126 2. Processes and Physics Controlling Precipitation Phase

127 Precipitation formed in the atmosphere is typically a solid in the mid-latitudes and its phase at  
128 the land surface is determined by whether it melts during its fall (Stewart et al., 2015). Most  
129 hydrologic models do not simulate atmospheric processes and specify precipitation phase based  
130 on surface conditions alone (see Section 4.1), ignoring phase transformations in the atmosphere.

131

132 Several important properties that influence phase changes in the atmosphere are not included in  
133 hydrological models (Feiccabrino et al., 2012), such as temperature and precipitation  
134 characteristics (Theriault and Stewart, 2010), stability of the atmosphere (Theriault and Stewart,  
135 2007), position of the 0 °C isotherm (Minder, 2010; Theriault and Stewart, 2010), interaction  
136 between hydrometeors (Stewart, 1992), and the atmospheric humidity profile (Harder and  
137 Pomeroy, 2013). The vertical temperature and humidity (represented by the mixing ratio) profile  
138 through which the hydrometeor falls typically consists of three layers, a top layer that is frozen  
139 ( $T < 0$  °C) in winter in temperate areas (Stewart, 1992), potentially a mixed layer with  $T > 0$  °C,  
140 and a surface layer that can be above or below 0 °C (Figure 2). The phase of precipitation at the  
141 surface partly depends on the phase reaching the top of the surface layer, which is defined as the

142 critical height. The temperature profile and depth of the surface layer controls the precipitation  
143 phase reaching the ground surface. For example, in Figure 2a, if rain reaches the critical height, it  
144 may reach the surface as rain or ice pellets depending on small differences in temperature in the  
145 surface layer (Theriault and Stewart, 2010). Similarly, in Figure 2b, if snow reaches the critical  
146 height, it may reach the surface as snow if the temperature in the surface layer is below freezing.  
147 However, in Figure 2c, when the surface layer temperatures are close to freezing and the mixing  
148 ratios are neither close to saturation or very dry the phase at the surface is not easily determined  
149 by the surface conditions alone.

150

151 In addition to strong dependence on the vertical temperature and humidity profiles, precipitation  
152 phase is also a function of fall rate and hydrometeor size because they affect energy exchange  
153 with the atmosphere (Theriault et al., 2010). Precipitation rate influences the precipitation phase;  
154 for example, a precipitation rate of  $10 \text{ mm h}^{-1}$  reduces the amount of freezing rain by a factor of  
155 three over a precipitation rate of  $1 \text{ mm h}^{-1}$  (Theriault and Stewart, 2010) because there is less  
156 time for exchange of turbulent heat with the hydrometeor. A solid hydrometeor that originates in  
157 the top layer and falls through the mixed layer can reach the surface layer as wet snow, sleet, or  
158 rain. This phase transition in the mixed layer is primarily a function of latent heat exchange  
159 driven by vapor pressure gradients and sensible heat exchange driven by temperature gradients.  
160 Temperature generally increases from the mixed layer to the surface layer causing sensible heat  
161 inputs to the hydrometeor. If these gains in sensible heat are combined with minimal latent heat  
162 losses resulting from low vapor pressure deficits, it is likely the hydrometeor will reach the  
163 surface layer as rain (Figure 2). However, vapor pressure in the mixed layer is often below  
164 saturation leading to latent energy losses and cooling of the hydrometeor coupled with diabatic  
165 cooling of the local atmosphere, which can produce snow or other forms of frozen precipitation  
166 at the surface even when temperatures are above  $0 \text{ }^{\circ}\text{C}$ . Likewise, surface energetics affect local  
167 atmospheric conditions and dynamics, especially in complex terrain. For example, melting of the  
168 snowpack can cause diabatic cooling of the local atmosphere and affect the phase of  
169 precipitation, especially when air temperatures are very close to  $0 \text{ }^{\circ}\text{C}$  (Theriault et al., 2012).  
170 Many conditions lead to a combination of latent heat losses and sensible heat gains by  
171 hydrometeors (Figure 2). Under these conditions it can be difficult to predict the phase of

172 precipitation without sufficient information about humidity and temperature profiles, turbulence,  
173 hydrometeor size, and precipitation intensity.

174

175 Stability of the atmosphere can also influence precipitation phase. Stability is a function of the  
176 vertical temperature structure which can be altered by vertical air movement and hence influence  
177 precipitation phase (Theriault and Stewart, 2007). Vertical air velocity changes the temperature  
178 structure by adiabatic warming or cooling due to pressure changes of descending and ascending,  
179 air parcels, respectively. These changes in temperature will generate under-saturated and  
180 supersaturated conditions in the atmosphere that can also alter the precipitation phase. Even a  
181 very weak vertical air velocity ( $< 10$  cm/s) significantly influences the phase and amount of  
182 precipitation formed in the atmosphere (Theriault and Stewart, 2007). The rain-snow line  
183 predicted by atmospheric models is very sensitive to these microphysics (Minder, 2010) and  
184 validating the microphysics across locations with complex physiography is challenging.  
185 Incorporation and validation of atmospheric microphysics is rarely achieved in hydrological  
186 applications (Feiccabrino et al., 2015).

187

### 188 3. Current Tools for Observing Precipitation Phase

#### 189 3.1 In situ observations

190 In situ observations refer to methods wherein a person or instrument onsite records precipitation  
191 phase. We identify 3 classes of approaches that are used to observe precipitation phase including  
192 1) direct observations, 2) coupled observations, and 3) proxy observations.

193

194 Direct observations simply involve a person on-site noting the phase of falling precipitation.  
195 Such data form the basis of many of the predictive methods that are widely used (Dai, 2008;  
196 Ding et al., 2014; U.S. Army Corps of Engineers, 1956). Direct observations are useful for  
197 “manned” stations such as those operated by the U.S. National Weather Service. Few research  
198 stations, however, have this benefit, particularly in many remote regions and in complex terrain.  
199 Direct observations are also limited in their temporal resolution and are typically reported only  
200 once per day, with some exceptions (Froidurot et al., 2014). Citizen scientist networks have  
201 historically provided valuable data to supplement primary instrumented observation networks.  
202 The National Weather Service Cooperative Observer Program  
203 (<http://www.nws.noaa.gov/om/coop/what-is-coop.html>, accessed 10/12/2016) is comprised of a

204 network of volunteers recording daily observations of temperature and precipitation, including  
205 phase. The NOAA National Severe Storms Laboratory used citizen scientist observations of rain  
206 and snow occurrence to evaluate the performance of the Multi-Radar Multi-Sensor (MRMS)  
207 system in the meteorological Phenomena Identification Near the Ground (mPING) project (Chen  
208 et al., 2015). The Colorado Climate Center initiated Community Collaborative Rain, Hail and  
209 Snow Network (CoCoRaHS) supplies volunteers with low cost instrumentation to observe  
210 precipitation characteristics, including phase, and enables observations to be reported on the  
211 project website (<http://www.cocorahs.org/>, accessed 10/12/2016). Although highly valuable,  
212 some limitations of this system include the imperfect ability of observers to identify mixed phase  
213 events and the temporal extent of storms, as well as the lack of observations in both remote areas  
214 and during low light conditions.

215  
216 Coupled observations link synchronous measurements of precipitation with secondary  
217 observations to indicate phase. Secondary observations can include photographs of surrounding  
218 terrain, snow depth measurements, and measurements of ancillary meteorological variables.  
219 Photographs of vertical scales emplaced in the snow have been used to estimate snow  
220 accumulation depth, which can then be coupled with precipitation mass to determine density and  
221 phase (Berris and Harr, 1987; Floyd and Weiler, 2008; Garvelmann et al., 2013; Hedrick and  
222 Marshall, 2014; Parajka et al., 2012). Mixed phase events, however, are difficult to quantify  
223 using coupled depth- and photographic-based techniques (Floyd and Weiler, 2008). Acoustic  
224 distance sensors, which are now commonly used to monitor the accumulation of snow (e.g. Boe,  
225 2013), have similar drawbacks in mixed phase events, but have been effectively applied to  
226 separate snow from rain (Rajagopal and Harpold, 2016). Meteorological information such as  
227 temperature and relative humidity can be used to compute the phase of precipitation measured by  
228 bucket-type gauges. Unfortunately, this approach generally requires incorporating assumptions  
229 about the meteorological conditions that determine phase (see section 4.1). Harder and Pomeroy  
230 (2013) used a comprehensive approach to determine the phase of precipitation. Every 15 minutes  
231 during their study period phase was determined by evaluating weighing bucket mass, tipping  
232 bucket depth, albedo, snow depth, and air temperature. Similarly, Marks et al. (2013) used a  
233 scheme based on co-located precipitation and snow depth to discriminate phase. A more  
234 involved expert decision making approach by L'hôte et al. (2005) was based on six recorded



235 meteorological parameters: precipitation intensity, albedo of the ground, air temperature, ground  
236 surface temperature, reflected long-wave radiation, and soil heat flux. The intent of most of these  
237 coupled observations was to develop datasets to evaluate PPM algorithms. However, if these  
238 observation systems were sufficiently simple they may have the potential to be applied  
239 operationally across larger meteorological monitoring networks encompassing complex terrain  
240 where snow comprises a large component of annual precipitation (Rajagopal and Harpold, 2016).

241  
242 Proxy observations measure geophysical properties of precipitation to infer phase. The hot plate  
243 precipitation gauge introduced by Rasmussen et al. (2012), for example, uses a heated thin disk  
244 to accumulate precipitation and then measures the amount of energy required to melt snow or  
245 evaporate liquid water. This technique, however, requires a secondary measurement of air  
246 temperature to determine if the energy is used to melt snow or only evaporate rain. Disdrometers  
247 measure the size and velocity of hydrometeors. Although the most common application of  
248 disdrometer data is to determine the drop size distribution (DSD) and other properties of rain, the  
249 phase of hydrometeors can be inferred by relating velocity and size to density. Some disdrometer  
250 technologies, which can be grouped into impact, imaging, and scattering approaches (Löffler-  
251 Mang et al., 1999), are better suited for describing snow than others. Impact disdrometers, first  
252 introduced by Joss and Waldvogel (1967), use an electromechanical sensor to convert the  
253 momentum of a hydrometeor into an electric pulse. The amplitude of the pulse is a function of  
254 drop diameter. Impact disdrometers have not been commonly used to measure solid precipitation  
255 due to the different functional relationships between drop size and momentum for solid and  
256 liquid precipitation. Imaging disdrometers use basic photographic principles to acquire images of  
257 the distribution of particles (Borrmann and Jaenicke, 1993; Knollenberg, 1970). The 2D Video  
258 Disdrometer (2DVD) described by Kruger and Krajewski (2002) records the shadows cast by  
259 hydrometeors onto photodetectors as they pass through two sheets of light. The shape of the  
260 shadows enables computation of particle size, and shadows are tracked through both light sheets  
261 to determine velocity. Although initially designed to describe liquid precipitation, recent work  
262 has shown that the 2DVD can be used to classify snowfall according to microphysical properties  
263 of single hydrometeors (Bernauer et al., 2016). The 2DVD has been used to classify known rain  
264 or snow events individually, but little work has been performed to distinguish between liquid and  
265 solid precipitation. Scattering disdrometers, or optical disdrometers, measure the extinction of

266 light passing between a source and a sensor (Hauser et al., 1984; Loffler-Mang et al., 1999). Like  
267 the other types, optical disdrometers were originally designed for rain, but have been periodically  
268 applied to snow (Battaglia et al., 2010; Lempio et al., 2007). In a comparison study by  
269 Caracciolo et al. (2006), the PARSIVEL optical disdrometer, originally described by Loffler-  
270 Mang et al. (1999) did not perform well against a 2DVD because of problems related to the  
271 detection of slow fall velocities for snow. It may be possible to use optical disdrometers to  
272 distinguish between rain, sleet, and snow based on the existence of distinct shapes of the size  
273 spectra for each precipitation type. More research on the relationship between air temperature  
274 and the size spectra produced by the optical disdrometer is needed (Lempio et al., 2007). In  
275 summary, disdrometers of various types are valuable tools for describing the properties of rain  
276 and snow, but require further testing and development to distinguish between rain and snow, as  
277 well as mixed phase events.

278

### 279 3.2 Ground-based remote sensing observations

280 Ground-based remote sensing observations have been available for several decades to detect  
281 precipitation phase using radar. Until recently, most ground-based radar stations were operated  
282 as conventional Doppler systems that transmit and receive radio waves with single horizontal  
283 polarization. Developments in dual polarization ground radar such as those that function as part  
284 of the U.S. National Weather Service NEXRAD network (NOAA, 2016), have resulted in  
285 systems that transmit radio signals with both horizontal and vertical polarizations. In general,  
286 ground-based remote sensing observation, either single or dual-pol, remain underutilized for  
287 detecting precipitation phase and are challenging to apply in complex terrain (Table 2).

288

289 Ground-based remote sensing of precipitation phase using single-polarized radar systems  
290 depends on detecting the radar bright band. Radio waves transmitted by the radar system, are  
291 scattered by hydrometeors in the atmosphere, with a certain proportion reflected back towards  
292 the radar antenna. The magnitude of the measured reflectivity ( $Z$ ) is related to the size and the  
293 dielectric constant of falling hydrometeors (White et al., 2002). Ice particles aggregate as they  
294 descend through the atmosphere and their dielectric constant increases, in turn increasing  $Z$   
295 measured by the radar, creating the bright band, a layer of enhanced reflectivity just below the  
296 elevation of the melting level (Lundquist et al., 2008). Therefore, bright band elevation can be

297 used as a proxy for the “snow level”, the bottom of the melting layer where falling snow  
298 transforms to rain (White et al., 2010; White et al., 2002).

299  
300 Doppler vertical velocity (DVV) is another variable that can be estimated from single-polarized  
301 vertically profiling radar. DVV gives an estimate of the velocity of falling particles; as  
302 snowflakes melt and become liquid raindrops, the fall velocity of the altered hydrometeors  
303 increases. When combined with reflectivity profiles, DVV helps reduce false positive detection  
304 of the bright band, which may be caused by phenomena other than snow melting to rain (White  
305 et al., 2002). First, DVV and Z are combined to detect the elevation of the bottom of the bright  
306 band. Then the algorithm searches for maximum Z above the bottom of the bright band and  
307 determines that to be the bright band elevation (White et al., 2002). However, a test of this  
308 algorithm on data from a winter storm over the Sierra Nevada found root mean square errors of  
309 326 to 457 m compared to ground observations when bright band elevation was assumed to  
310 represent the surface transition from snow to rain (Lundquist et al., 2008). Snow levels in  
311 mountainous areas, however, may also be overestimated by radar profiler estimates if they are  
312 unable to resolve spatial variations close to mountain fronts, since snow levels have been noted  
313 to persistently drop on windward slopes (Minder and Kingsmill, 2013). Despite the potential  
314 errors, the elevation of maximum Z may be a useful proxy variable for snow level in  
315 hydrometeorological applications in mountainous watersheds because maximum Z will always  
316 occur below the freezing level (Lundquist et al., 2008; White et al., 2010)

317  
318 Few published studies have explored the value of bright band-derived phase data for hydrologic  
319 modeling. Maurer and Mass (2006) compared the melting level from vertically pointing radar  
320 reflectivity against temperature-based methods to assess whether the radar approach could  
321 improve determination of precipitation phase at the ground level. In that study, the altitude of the  
322 top of the bright band was detected and applied across the study basin. Frozen precipitation was  
323 assumed to be falling in model pixels above the altitude of the melting level and liquid  
324 precipitation was assumed to be falling in pixels below the altitude of the melting layer (Maurer  
325 and Mass, 2006). Maurer and Mass (2006) found that incorporating radar-detected melting layer  
326 altitude improved streamflow simulation results. A similar study that used bright band altitude to  
327 classify pixels according to surface precipitation type was not as conclusive; bright band altitude

328 data did not improve hydrologic model simulation results over those based on a temperature  
329 threshold (Mizukami et al., 2013). Also, the potential of the method is limited to the availability  
330 of vertically pointing radar; in complex, mountainous terrain the ability to estimate melting level  
331 becomes increasingly challenging with distance from the radar.

332  
333 Dual-polarized radar systems generate more variables than traditional single-polarized systems.  
334 These polarimetric variables include differential reflectivity, reflectivity difference, the  
335 correlation coefficient, and specific differential phase. Polarimetric variables respond to  
336 hydrometeor properties such as shape, size, orientation, phase state, and fall behavior and can be  
337 used to assign hydrometeors to specific categories (Chandrasekar et al., 2013; Grazioli et al.,  
338 2015), or to improve bright band detection (Giangrande et al., 2008).

339  
340 Various hydrometeor classification algorithms have been applied to X-, C- and S-band  
341 wavelengths. Improvements in these algorithms over recent years have seen hydrometeor  
342 classification become an operational meteorological product (see Grazioli et al., 2015 for an  
343 overview). For example, the U.S. National Severe Storms Laboratory (NSSL) developed a fuzzy-  
344 logic hydrometeor classification algorithm for warm-season convective weather (Park et al.,  
345 2009) and this algorithm has also been tested for cold-season events (Elmore, 2011). Its skill was  
346 tested against surface observations of precipitation type but the algorithm did not perform well in  
347 classifying winter precipitation because it could not account for re-freezing of hydrometeors  
348 below the melting level (Figure 2, Elmore, 2011). Unlike warm season convective precipitation,  
349 the freezing level during a cold-season precipitation event can vary spatially. This phenomenon  
350 has prompted the use of polarimetric variables to first detect the melting layer, and then classify  
351 hydrometeors (Boodoo et al., 2010; Thompson et al., 2014). Although there has been some  
352 success in developing two-stage cold-season hydrometeor classification algorithms, there is little  
353 in the published literature that explores the potential contributions of these algorithms for  
354 partitioning snow and rain for hydrological modeling.

355  
356 **3.3 Space-based remote sensing observations**  
357 Spaceborne remote sensing observations typically use passive or active microwave sensors to  
358 determine precipitation phase (Table 2). Many of the previous passive microwave systems were

359 challenged by coarse resolutions and difficulties retrieving snowfall over snow-covered areas.  
360 More recent active microwave systems have advantage for detecting phase in terms of accuracy  
361 and spatial resolution, but remain largely unverified. Table 2 provides an overview of these  
362 space-based remote sensing technologies that are described in more detail below.

363  
364 Passive microwave radiometers detect microwave radiation emitted by the Earth's surface or  
365 atmosphere. Passive microwave remote sensing has potential for discriminating between rainfall  
366 and snowfall because microwave radiation emitted by the Earth's surface propagates through all  
367 but the densest precipitating clouds, meaning that radiation at microwave wavelengths directly  
368 interacts with hydrometeors within clouds (Olson et al., 1996; Ardanuy, 1989). However, the  
369 remote sensing of precipitation in microwave wavelengths and the development of operational  
370 algorithms is dominated by research focused on rainfall (Arkin and Ardanuy, 1989); by  
371 comparison, snowfall detection and observation has received less attention (Noh et al., 2009;  
372 Kim et al., 2008). This is partly explained by examining the physical processes within clouds that  
373 attenuate the microwave signal. Raindrops emit low levels of microwave radiation increasing the  
374 level of radiance measured by the sensor; in contrast, ice hydrometeors scatter microwave  
375 radiation, decreasing the radiance measured by a sensor (Kidd and Huffman, 2011). Land  
376 surfaces have a much higher emissivity than water surfaces, meaning that emission-based  
377 detection of precipitation is challenging over land because the high microwave emissions mask  
378 the emission signal from raindrops (Kidd, 1998; Kidd and Huffman, 2011). Thus, scattering-  
379 based techniques using medium to high frequencies are used to detect precipitation over land.  
380 Moreover, microwave observations at higher frequencies ( $> 89$  GHz) have been shown to  
381 discriminate between liquid and frozen hydrometeors (Wilheit et al., 1982).

382  
383 Retrieving snowfall over land areas from spaceborne microwave sensors can be even more  
384 challenging than for liquid precipitation because existing snow cover increases microwave  
385 emission. Depression of the microwave signal caused by scattering from airborne ice particles  
386 may be obscured by increased emission of microwave radiation from the snow covered land  
387 surface. Kongoli et al. (2003) demonstrated an operational snowfall detection algorithm that  
388 accounts for the problem of existing snow cover. This group used data from the Advanced  
389 Microwave Sounding Unit-A (AMSU-A), a 15-channel atmospheric temperature sounder with a

390 single high frequency channel at 89 GHz), and AMSU-B, a 5-channel high frequency microwave  
391 humidity sounder. Both sensors were mounted on the NOAA-16 and -17 polar-orbiting satellites.  
392 While the algorithm worked well for warmer, opaque atmospheres, it was found to be too noisy  
393 for colder, clear atmospheres. Additionally, some snowfall events occur under warmer conditions  
394 than those that were the focus of the study (Kongoli et al., 2003). Kongoli et al. (2015) further  
395 adapted their methodology for the Advanced Technology Microwave Sounder (ATMS - onboard  
396 the polar-orbiting Suomi National Polar-orbiting Partnership satellite) a descendant of the  
397 AMSU sounders. The latest algorithm assesses the probability of snowfall using the logistic  
398 regression and the principal components of seven high frequency bands at 89 GHz and above. In  
399 testing, the Kongoli et al. (2015) algorithm has shown skill in detecting snowfall both at variable  
400 rates and when snowfall is lighter and occurs in colder conditions. An alternative algorithm by  
401 Noh et al., 2009 used physically-based, radiative transfer modeling in an attempt to improve  
402 snowfall retrieval over land. In this case, radiative transfer modeling was used to construct an *a*  
403 *priori* database of observed snowfall profiles and corresponding brightness temperatures. The  
404 radiative transfer procedure yields likely brightness temperatures from modeling how ice  
405 particles scatter microwave radiation at different wavelengths. A Bayesian retrieval algorithm  
406 was then used to estimate snowfall over land by comparing measurements of brightness  
407 temperature with modeled brightness temperature (Noh et al., 2009). The algorithm was tested  
408 during the early and late winter for heavier snowfall events. Late winter retrievals indicated that  
409 the algorithm overestimated snowfall over surfaces with significant snow accumulation.

410

411 While results have been promising, the spatial resolution at which ATMS and other passive  
412 microwave data are acquired is very coarse (15.8 to 74.8 km at nadir), making passive  
413 microwave approaches more applicable for regional to continental scales. Temporal resolution of  
414 the data acquisition is another challenge. AMSU instruments are mounted on 8 satellites; the  
415 related ATMS is mounted on a single satellite and planned for two additional satellites.

416 However, the satellites are polar-orbiting, not geostationary, so it is probable that a precipitation  
417 event could occur outside the field of view of one of the instruments.

418

419 Spaceborne active microwave or radar sensors measure the backscattered signal from pulses of  
420 microwave energy emitted by the sensor itself. Much like the ground based radar systems, the

421 propagated microwave signal interacts with liquid and solid particles in the atmosphere and the  
422 degree to which the measured return signal is attenuated provides information on the  
423 atmospheric constituents. The advantage offered by spaceborne radar sensors over passive  
424 microwave is the capability to acquire more detailed sampling of the vertical profile of the  
425 atmosphere (Kulie and Bennartz, 2009). The first spaceborne radar capable of observing  
426 snowfall is the Cloud Profiling Radar (CPR) onboard CloudSat (2006 – present). The CPR  
427 operates at 94 GHz with an along-track (or vertical) resolution of ~1.5 km. Retrieval of dry  
428 snowfall rate from CPR measurements of reflectivity have been shown to correspond with  
429 estimates of snowfall from ground-based radar at elevations of 2.6 and 3.6 km above mean sea  
430 level (Matrosov et al., 2008). Estimates at lower elevations, especially those in the lowest 1 km,  
431 are contaminated by ground clutter. Alternative approaches, combining CPR data with ancillary  
432 data have been formulated to account for this challenge (Kulie and Bennartz, 2009; Liu, 2008).  
433 Known relationships between CPR reflectivity data and the scattering properties of non-spherical  
434 ice crystals are used to derive snowfall at a given elevation above mean sea level; below this  
435 elevation a temperature threshold derived from surface data is used to discriminate between rain  
436 and snow events. Liu (2008) used  $<2$  °C as the snow/rain threshold, whereas Kulie and Bennartz  
437 (2009) used 0 °C as the snow/rain threshold. Temperature thresholds have been the subject of  
438 much research and debate for discriminating precipitation phase, as is further discussed in  
439 section 4.1.

440  
441 CloudSat is part of the A-train or afternoon constellation of satellites, which includes Aqua, with  
442 the Moderate Resolution Imaging Spectrometer (MODIS) and the Cloud–Aerosol Lidar and  
443 Infrared Pathfinder Satellite Observations (CALIPSO) spacecraft with cloud-profiling Lidar. The  
444 sensors onboard A-train satellites provided the unique combination of data to create an  
445 operational snow retrieval product. The CPR Level 2 snow profile product (2C-SNOW-  
446 PROFILE) uses vertical profile data from the CPR, input from MODIS and the cloud profiling  
447 radar, as well as weather forecast data to estimate near surface snowfall (Kulie et al., 2016;  
448 Wood et al., 2013). The performance of 2C-SNOW-PROFILE was tested by Cao et al. (2014).  
449 This group found the product worked well in detecting light snow but performed less  
450 satisfactorily under conditions of moderate to heavy snow because of the non-stationary effects  
451 of attenuation on the returned radar signal.

452  
453 The launch of the Global Precipitation Mission (GPM) core observatory in February 2014 holds  
454 promise for the future deployment of operational snow detection products. Building on the  
455 success of the Tropical Rainfall Monitoring Mission (TRMM), the GPM core observatory  
456 sensors include precipitation radar (DPR) and microwave imager (GMI). The GMI has two  
457 millimeter wave channels (166 and 183 GHz) that are specifically designed to detect and retrieve  
458 light rain and snow precipitation. These are more advanced than the sensors onboard the TRMM  
459 spacecraft and permit better quantification of the physical properties of precipitating particles,  
460 particularly over land at middle to high latitudes (Hou et al., 2014). Algorithms for the GPM  
461 mission are still under development, and is partly being driven by data collected during the GPM  
462 Cold Season Experiment (GCPEX) (Skofronick-Jackson et al., 2015). Using airborne sensors to  
463 simulate GPM and DPR measurements, one of the questions that the GCPEX hoped to address  
464 concerned the potential capability of data from the DPR and GMI to discriminate falling snow  
465 from rain or clear air (Skofronick-Jackson et al., 2015). The initial results reported by the GCPEX  
466 study echo some of the challenges recognized for ground-based single polarized radar detection  
467 of snowfall. The relationship between radar reflectivity and snowfall is not unique. For the GPM  
468 mission, it will be necessary to include more variables from dual frequency radar measurements,  
469 multiple frequency passive microwave measurements, or a combination of radar and passive  
470 microwave measurements (Skofronick-Jackson et al., 2015).

#### 471 472 4. Current Tools for Predicting Precipitation Phase

##### 473 4.1 Prediction Techniques from Ground-Based Observations

474 Discriminating between solid and liquid precipitation is often based on a near-surface air  
475 temperature threshold (Martinec and Rango, 1986; U.S. Army Corps of Engineers, 1956; L'hôte et  
476 al., 2005). Four prediction methods have been developed that use near-surface air temperature  
477 for discriminating precipitation phase: 1) static threshold, 2) linear transition, 3) minimum and  
478 maximum temperature, and 4) sigmoidal curve (Table 1). A static temperature threshold applies  
479 a single temperature value, such as mean daily temperature, where all of the precipitation above  
480 the threshold is rain, and all below that threshold is snow. Typically this threshold temperature is  
481 near 0 °C (Lynch-Stieglitz, 1994; Motoyama, 1990), but was shown to be highly variable across  
482 both space and time (Kienzle, 2008; Motoyama, 1990; Braun, 1984; Ye et al., 2013). For



483 example, Rajagopal and Harpold (2016) optimized a single temperature threshold at Snow  
484 Telemetry (SNOTEL) sites across the western U.S. to show regional variability from -4 to 3 °C  
485 (Figure 3). A second discrimination technique is to linearly scale the proportion of snow and rain  
486 between a temperature for all rain ( $T_{\text{rain}}$ ) and a temperature for all snow ( $T_{\text{snow}}$ ) (Pipes and Quick,  
487 1977;McCabe and Wolock, 2010;Tarboton et al., 1995). Linear threshold models have been  
488 parameterized slightly differently across studies, e.g.:  $T_{\text{snow}} = -1.0$  °C,  $T_{\text{rain}} = 3.0$  °C (McCabe and  
489 Wolock, 2010),  $T_{\text{snow}} = -1.1$  °C and  $T_{\text{rain}} = 3.3$  °C (Tarboton et al., 1995), and  $T_{\text{snow}} = 0$  °C and  $T_{\text{rain}}$   
490  $= 5$  °C (McCabe and Wolock, 1999b). A third technique specifies a threshold temperature based  
491 on daily minimum and maximum temperatures to classify rain and snow, respectively, with a  
492 threshold temperature between the daily minimum and maximum producing a proportion of rain  
493 and snow (Leavesley et al., 1996). This technique can have a time-varying temperature threshold  
494 or include a  $T_{\text{rain}}$  that is independent of daily maximum temperature. A fourth technique applies a  
495 sigmoidal relationship between mean daily (or sub daily) temperature and the proportion or  
496 probability of snow versus rain. For example, one method derived for southern Alberta, Canada  
497 employs a curvilinear relationship defined by two variables, a mean daily temperature threshold  
498 where 50% of precipitation is snow, and a temperature range where mixed-phase precipitation  
499 can occur (Kienzle, 2008). Another sigmoidal-based empirical model identified a hyperbolic  
500 tangent function defined by four parameters to estimate the conditional snow (or rain) frequency  
501 based on a global analysis of precipitation phase observations from over 15,000 land-based  
502 stations (Dai, 2008). Selection between temperature-based techniques is typically based on  
503 available data, with a limited number of studies quantifying their relative accuracy for  
504 hydrological applications (Harder and Pomeroy, 2014).

505  
506 Several studies have compared the accuracy of temperature-based PPM to one another and/or  
507 against an independent validation of precipitation phase. Sevruk (1984) found that only about  
508 68% of the variability in monthly observed snow proportion in Switzerland could be explained  
509 by threshold temperature based methods near 0 °C. An analysis of data from fifteen stations in  
510 southern Alberta, Canada with an average of >30 years of direct observations noted over-  
511 estimations in the mean annual snowfall for static threshold (8.1%), linear transition (8.2%),  
512 minimum and maximum (9.6%), and sigmoidal transition (7.1%) based methods (Kienzle, 2008).  
513 An evaluation of PPM at three sites in the Canadian Rockies by Harder and Pomeroy (2013)

514 found the largest percent error to occur using a static threshold (11% to 18%), followed by linear  
515 relationships (-8% to 11%), followed by a sigmoidal relationships (-3 to 11%). Another study  
516 using 824 stations in China with >30 years of direct observations found accuracies of 51.4%  
517 using a static 2.2 °C threshold and 35.7% to 47.4% using linear temperature-based thresholds  
518 (Ding et al., 2014). Lastly, for multiple sites across the rain-snow transition in southwestern  
519 Idaho, static temperature thresholds produced the lowest proportion (68%) whereas a linear-  
520 based model produced the highest proportion (75%) of snow, respectively (Marks et al., 2013).  
521 Generally these accuracy assessments demonstrated that static threshold methods produced the  
522 greatest errors, whereas sigmoidal relationships produced the smallest errors, although variations  
523 to this general rule existed across sites.

524

525 Near surface humidity also influences precipitation phase (see Section 2). Three humidity-  
526 dependent precipitation phase identification methods are found in the literature: 1) dewpoint  
527 temperature ( $T_d$ ), 2) wet bulb temperature ( $T_w$ ), and 3) psychrometric energy balance. The  
528 dewpoint temperature is the temperature at which an air parcel with a fixed pressure and  
529 moisture content would be saturated. In one approach to account for measurement and  
530 instrument calibration uncertainties of  $\pm 0.25$  °C each,  $T_d$  and  $T_w$  below -0.5 °C was assumed to  
531 be all snow and above +0.5 °C all rain, with a linear relationship between the two being a  
532 proportional mix of snow and rain (Marks et al., 2013).  $T_d$  of 0.0 °C performed consistently  
533 better than  $T_a$  in one study by Marks et al. (2001) while a  $T_d$  of 0.1 °C for multiple stations in  
534 Sweden was less accurate than a  $T_a$  of 1.0 °C (Feiccabrino et al., 2013). The wet or ice bulb  
535 temperature ( $T_w$ ) is the temperature at which an air parcel would become saturated by  
536 evaporative cooling in the absence of other sources of sensible heat, and is the lowest  
537 temperature that falling precipitation can reach. Few studies have investigated the feasibility of  
538  $T_w$  for precipitation phase prediction (Olsen, 2003; Ding et al., 2014; Marks et al., 2013).  $T_w$   
539 significantly improved prediction of precipitation phase over  $T_a$  at 15-minute time steps, but only  
540 marginally improved prediction at daily time steps (Marks et al., 2013). Ding et al. (2014)  
541 developed a sigmoidal phase probability curve based on  $T_w$  and elevation that outperformed  $T_a$   
542 threshold-based methods across a network of sites in China. Conceptually, the hydrometeor  
543 temperature ( $T_i$ ) is similar to  $T_w$  but is calculated using the latent heat and vapor density gradient.

544 Use of computed  $T_i$  value significantly improved precipitation phase estimates over  $T_a$ ,  
545 particularly as time scales approached one day (Harder and Pomeroy, 2013).

546

547 There has been limited validation of humidity-based precipitation phase prediction techniques  
548 against ground-truth observations. Ding et al. (2014) showed that a method based on  $T_w$  and  
549 elevation increased accuracy by 4.8% to 8.9% over several temperature-based methods. Their  
550 method was more accurate than a simpler  $T_w$  based method by (Yamazaki, 2001). Feiccabrino et  
551 al. (2013) showed that  $T_d$  misclassified 3.0% of snow and rain (excluding mixed phased  
552 precipitation), whereas  $T_a$  only misclassified 2.4%. Ye et al. (2013) found  $T_d$  less sensitive to  
553 phase discrimination under diverse environmental conditions and seasons than  $T_a$ . Froidurot et  
554 al. (2014) evaluated several techniques with a critical success index (CSI) at sites across  
555 Switzerland to show the highest CSI were associated with variables that included  $T_w$  or relative  
556 humidity (CSI=84%-85%) compared to  $T_a$  (CSI=78%). Marks et al. (2013) evaluated the time at  
557 which phase transitioned from snow to rain against field observations across a range of  
558 elevations and found that  $T_d$  most closely predicted the timing of phase change, whereas both  $T_a$   
559 and  $T_w$  estimated earlier phase changes than observed. Harder and Pomeroy (2013) compared  $T_i$   
560 with field observations and found that error was <10% when  $T_i$  was allowed to vary with each  
561 daily time-step and >10% when  $T_i$  was fixed at 0 °C. The  $T_i$  accuracy increased appreciably (i.e.  
562 5%-10% improvement) when the temporal resolution was decreased from daily to hourly or 15-  
563 minute time steps. The validation studies consistently showed improvements in accuracy by  
564 including humidity over PPM based only on temperature.

565

566 Hydrological models employ a variety of techniques for phase prediction using ground based  
567 observations (Table 1). All discrete hydrological models (i.e. not coupled to an atmospheric  
568 model) investigated used temperature based thresholds that did not consider the near-surface  
569 humidity. Moreover, most models use a single static temperature threshold, which was  
570 consistently shown to produce lower accuracy than multiple temperature methods. Hydrological  
571 models that are coupled to atmospheric models were more able to consider important controls on  
572 precipitation phase, such as humidity and atmospheric profiles. This compendium of model PPM  
573 highlights the current shortcomings in phase prediction in conventional discrete hydrological  
574 models.

575

## 576 4.2 Prediction Techniques Incorporating Atmospheric Information

577 While many hydrologic models have their own formulations for determining precipitation phase  
578 at the ground, it is also possible to initialize hydrologic models with precipitation phase fraction,  
579 intensity, and volume from numerical weather simulation model output. Here we discuss the  
580 limitations of precipitation phase simulation inherent to WRF (Kaplan et al., 2012; Skamarock et  
581 al., 2008) and other atmospheric simulation models. The finest scale spatial resolution employed  
582 in atmospheric simulation models is  $\sim 1$  km and these models generate data at hourly or finer  
583 temporal resolutions. Regional climate models (RCM) and global climate models (GCM) are  
584 typically coarser than local mesoscale models. The physical processes driving both the removal  
585 of moisture from the air and the precipitation phase (Section 2) occur at much finer spatial and  
586 temporal resolutions in the real atmosphere than models typically resolve, i.e.  $< 1$  km. As with all  
587 numerical models, the representation of sub-grid scale processes requires parameterization. At  
588 typical scales considered, characterization of mixed phase processes within a condensing cloud  
589 depends on both cloud microphysics and kinematics of the surrounding atmosphere. Replicating  
590 cloud physics at the multi-kilometer scale requires empiricism. The 30+ cloud microphysics  
591 parameterization options in the research version of WRF (Skamarock et al., 2008) vary in the  
592 number of classes described (cloud ice, cloud liquid, snow, rain, graupel, hail, etc.), and may or  
593 may not accurately resolve changes in hydrometeor phase and horizontal spatial location (due to  
594 wind) during precipitation. All microphysical schemes predict cloud water and cloud ice based  
595 on internal cloud processes that include a variety of empirical formulations or even simple  
596 lookup tables. These schemes vary greatly in their accuracy with “mixed phase” schemes  
597 generally producing the most accurate simulations of precipitation phase in complex terrain  
598 where much of the water is supercooled (Lin, 2007; Reisner et al., 1998; Thompson et al., 2004;  
599 Thompson et al., 2008; Morrison et al., 2005; Zängl, 2007; Kaplan et al., 2012). Comprehensive  
600 validation of the microphysical schemes over different land surface types (e. g. warm maritime,  
601 flat prairie, etc.) with a focus on different snowfall patterns is lacking. In particular, in transition  
602 zones between mountains and plains or along coastlines, the complexity of the microphysics  
603 becomes even more extreme due the dynamics and interactions of differing air masses with  
604 distinct characteristics. The autoconversion and growth processes from cloud water or ice to  
605 hydrometeors contain a strong component of empiricism, in particular the nucleation media and

606 their chemical composition. Different microphysical parameterizations lead to different spatial  
607 distributions of precipitation and produce varying vertical distributions of hydrometeors  
608 (Gilmore et al., 2004). Regardless, precipitation rates for each grid cell are averages requiring  
609 hydrological modelers to consider the effects of elevation, aspect, etc. in resolving precipitation  
610 phase fractions for finer-scale models.

611

612 Numerical models that contain sophisticated cloud microphysics schemes allow assimilation of  
613 additional remote sensing data beyond conventional synoptic/large scale observations (balloon  
614 data). This is because the coarse spatial and temporal nature of radiosonde data results in the  
615 atmosphere being sensed imperfectly/incompletely compared with the scale of motion that  
616 weather simulation models can numerically resolve. These observational inadequacies are  
617 exacerbated in complex terrain, where precipitation phase fraction can vary on small scales but  
618 radar can be blocked by topography and therefore, rendered useless in the model initialization.  
619 Accurate generation of liquid and frozen precipitation from vapor requires accurate depiction of  
620 initial atmospheric moisture conditions (Kalnay and Cai, 2003; Lewis et al., 2006). In  
621 acknowledgement of the difficulty and uncertainty of initializing numerical simulation models,  
622 atmospheric modelers use the term “bogusing” to describe incorporation of individual  
623 observations at a point location into large scale initial conditions in an effort to enhance the  
624 accuracy of the simulation (Eddington, 1989). They also employ complex assimilation  
625 methodologies to force the early period of the model solutions during the time integration  
626 towards fine scale observations (Kalnay and Cai, 2003; Lewis et al., 2006). These asynoptic or  
627 fine scale data sources often substantially improve the accuracy of the simulations as time  
628 progresses.

629

630 Hydrologists are increasingly using output from atmospheric models to drive hydrologic models  
631 from daily to climate or multi-decadal timescales (Tung and Haith, 1995; Pachauri, 2002; Wood  
632 et al., 2004; Rojas et al., 2011; Yucel et al., 2015). These atmospheric models suffer from the  
633 same data paucity and scale issues that likewise challenge the implementation and validation of  
634 hydrologic models. Uncertainties in their output, including precipitation volume and phase,  
635 begins with the initialization of the atmospheric model from measurements, increases with model  
636 choice and microphysics as well as turbulence parameterizations, and is a strong function of the

637 scale of the model. The significance of these uncertainties varies by application, but should be  
638 acknowledged. Furthermore, these uncertainties are highly variable in character and magnitude  
639 from day to day and location to location. Thus, there has been very little published concerning  
640 how well atmospheric models predict precipitation phase. Finally, lack of ground measurements  
641 leaves hydrologists with no means to assess and validate atmospheric model predictions.

642

## 643 5. Research Gaps

644 The incorrect prediction of precipitation phase leads to cascading effects on hydrological  
645 modeling (Figure 1). Meeting the challenge of accurately predicting precipitation phase requires  
646 the closing of several critical research gaps (Figure 4). Perhaps the most pressing challenge for  
647 improving PPM is developing and employing new and improved sources of data. However, new  
648 data sources will not yield much benefit without effective incorporation of data into predictive  
649 models (Figure 4). Additionally, both the scientific and management communities lack data  
650 products that can be readily understood and broadly used. Addressing these research gaps  
651 requires simultaneous engagement both within and between the hydrology and atmospheric  
652 observation and modeling communities. Changes to atmospheric temperature and humidity  
653 profiles from regional climate change will likely challenge conventional precipitation phase  
654 prediction in ways that demand additional observations and improved forecasts.

655

### 656 5.1 Conduct focused field campaigns

657 Intensive field campaigns are extremely effective approaches to address fundamental research  
658 gaps focused on the discrimination between rain, snow, and mixed-phase precipitation at the  
659 ground by providing opportunities to test novel sensors, and detailed datasets to develop remote  
660 sensing retrieval algorithms, and improve PPM estimation methods. The recent Global  
661 Precipitation Measurement (GPM) Cold Season Precipitation Experiment (GCPEX) is an  
662 example of such a campaign in non-complex terrain where simultaneous observations using  
663 arrays of both airborne and ground-based sensors were used to measure and characterize both  
664 solid and liquid precipitation (e.g. Skofronick-Jackson et al., 2015). Similar intensive field  
665 campaigns are needed in complex terrain that is frequently characterized by highly dynamic and  
666 spatially variable hydrometeorological conditions. Such campaigns are expensive to conduct, but  
667 can be implemented as part of operational nowcasting to develop rich data resources to advance

668 scientific understanding as was very effectively done during the Vancouver Olympic Games in  
669 2010 (Isaac et al., 2014; Joe et al., 2014). The research community should utilize existing  
670 datasets and capitalize on similar opportunities and expand environmental monitoring networks  
671 to simultaneously advance both atmospheric and hydrological understanding, especially in  
672 complex terrain spanning the rain-snow transition zone.

673

## 674 5.2 Incorporate humidity information

675 Atmospheric humidity affects the energy budget of falling hydrometeors (Section 4.1), but is  
676 rarely considered in precipitation phase prediction. The difficulty in incorporating humidity  
677 mainly arises from a lack of observations, both as point measurements and distributed gridded  
678 products. For example, while some reanalysis products have humidity information (i.e. National  
679 Centers for Environmental Prediction, NCEP reanalysis) they are at spatial scales (i.e. > 1  
680 degree) too coarse for resolving precipitation phase in complex topography. Addition of high-  
681 quality aspirated humidity sensors at snow monitoring stations, such as the SNOTEL network,  
682 would advance our understanding of humidity and its effects on precipitation phase in the  
683 mountains. Because dry air masses have regional variations controlled by storm tracks and  
684 proximity to water bodies, sensitivity of precipitation phase to humidity variations driven by  
685 regional warming remains relatively unexplored.

686

687 Although humidity datasets are relatively rare in mountain environments, some gridded data  
688 products exist that can be used to investigate the importance of humidity information. Most  
689 interpolated gridded data products either do not include any measure of humidity (e.g. Daymet or  
690 WorldClim) or use daily temperature measurements to infer humidity conditions (e.g. PRISM).  
691 In complex terrain, air temperature can also vary dramatically at relatively small scales from  
692 ridgetops to valley bottoms due to cold air drainage (Whiteman et al., 1999) and hence can  
693 introduce errors into inferential techniques such as these. Potentially more useful are data  
694 assimilation products, such as NLDAS-2, that provide humidity and temperature values at 1/8<sup>th</sup>  
695 of a degree scale over the continental U.S. In addition, several data reanalysis products are often  
696 available at 1 to 3 year lags from present, including NCEP/NCAR, NARR, and the 20<sup>th</sup> Century  
697 reanalysis. Given the relatively sparse observations of humidity in mountain environments, the  
698 accuracy of gridded humidity products is rarely rigorously evaluated (Abatzoglou, 2013). More

699 work is needed to understand the added skill provided by humidity datasets for predicting  
700 precipitation phase and its distribution over time and space.

701

## 702 5.2 Incorporate atmospheric information

703 We echo the call of Feiccabrino et al. (2015) for greater incorporation of atmospheric  
704 information into phase prediction and additional verification of the skill in phase prediction  
705 provided by atmospheric information.

706

707 Several avenues exist to better incorporate atmospheric information into precipitation phase  
708 prediction, including direct observations, remote sensing observations, and model products.  
709 Radiosonde measurements made daily at many airports and weather forecasting centers have  
710 shown some promise for supplying atmospheric profiles of temperature and humidity (Froidurot  
711 et al., 2014). However, these data are only useful to initialize the larger scale structure of  
712 temperature and water vapor, and may not capture local-scale variations in complex terrain. It is  
713 also their lack of temporal and spatial frequency that prevents their use in accurate precipitation  
714 phase prediction, which is inherently a mesoscale problem, i.e., scales of motion  $<100$  km.  
715 Atmospheric information on the bright-band height from Doppler radar has been utilized for  
716 predicting the altitude of the rain-snow transition (Lundquist et al., 2008; Minder, 2010), but has  
717 rarely been incorporated into hydrological modeling applications (Maurer and Mass, 2006;  
718 Mizukami et al., 2013). In addition to atmospheric observations, modeling products that  
719 assimilate observations or are fully physically-based may provide additional information for  
720 precipitation phase prediction. Numerous reanalysis products (described in Section 2.2) provide  
721 temperature and humidity at different pressure levels within the atmosphere. To our knowledge,  
722 information from reanalysis products has yet to be incorporated into precipitation phase  
723 prediction for hydrological applications. Bulk microphysical schemes used by meteorological  
724 models (i.e. Weather Research and Forecasting WRF model) provide a physically-based estimate  
725 of precipitation phase. These schemes capture a wide-variety of processes, including  
726 evaporation, sublimation, condensation, and aggradation, and output between two and ten  
727 precipitation types. Historically, meteorological models have not been run at spatial scales  
728 capable of resolving convective dynamics (e.g.  $<2$  km), which can exacerbate error in  
729 precipitation phase prediction in complex terrain with a moist neutral atmosphere. Coarse



730 meteorological models also struggle to produce pockets of frozen precipitation from advection of  
731 moisture plumes between mountain ranges and cold air wedged between topographic barriers.  
732 However, reduced computational restrictions on running these models at finer spatial scales and  
733 over large geographic extents (Rasmussen et al., 2012) are enabling further investigations into  
734 precipitation phase change under historical and future climate scenarios. This suggests that finer  
735 dynamical downscaling is necessary to resolve precipitation phase which is consistent with  
736 similar work attempting to resolve winter precipitation amount in complex terrain (Gutmann et  
737 al., 2012). A potentially impactful area of research is to integrate this information into novel  
738 approaches to improve precipitation phase prediction skill.

739

### 740 5.3 Disdrometer networks operating at high temporal resolutions

741 An increase in the types and reliability of disdrometers over the last decade has provided a new  
742 suite of tools to more directly measure precipitation phase. Despite this new potential resource  
743 for distinguishing snow and rain, very limited deployments of disdrometers have occurred at the  
744 scale necessary to improve hydrologic modeling and rain-snow elevation estimates. The lack of  
745 disdrometer deployment likely arises from a number of potential limitations: 1) known issues  
746 with accuracy, 2) cost of these systems, and 3) power requirements needed for heating elements.  
747 These limitations are clearly a factor in procuring large networks and deploying disdrometers in  
748 complex terrain that is remote and frequently difficult to access. However, we advise that  
749 disdrometers offer numerous benefits that cannot be substituted with other measurements: 1)  
750 they operate at fine temporal scales, 2) they operate in low light conditions that limit other direct  
751 observations, and 3) they provide land surface observations rather than precipitation phase in the  
752 atmosphere (as compared to more remote methods). Moreover, improvements in disdrometer and  
753 power supply technologies that address these limitations would remove restrictions on increased  
754 disdrometer deployment.

755

756 Transects of disdrometers spanning the rain-snow elevations of key mountain areas could add  
757 substantially to both prediction of precipitation phase for modeling purposes, as well as  
758 validating typical predictive models. We advocate for transects over key mountain passes where  
759 power is generally available and weather forecasts for travel are particularly important. In  
760 addition, co-locating disdrometers at long-term research stations where precipitation phase

761 observations could be tied to micro-meteorological and hydrological observations has distinct  
762 advantages. These areas often have power supplies and instrumentation expertise to operate and  
763 maintain disdrometer networks.

764

#### 765 5.4 Compare different indirect phase measurement methods

766 There is an important need to evaluate the accuracy of different PPM to assess tradeoffs between  
767 model complexity and skill (Figure 4). Given the potential for several types of observations to  
768 improve precipitation phase prediction (section 5.1-5.3), quantifying the relative skill provided  
769 by these different lines of evidence is a critical research gap. Although assessing relative  
770 differences between methods is potentially informative, comparison to ground truth  
771 measurements is critical for assessing accuracy. Disdrometer measurements and video imaging  
772 (Newman et al., 2009) are ideal ground truthing methods that can be employed at fine time steps  
773 and under a variety of conditions (section 5.3). Less ideal for accuracy assessment studies are  
774 direct visual observations that are harder to collect at fine time steps and in low light conditions.  
775 Similarly, employing coupled observations of precipitation and snow depth has been used to  
776 assess accuracy of different precipitation phase prediction methods (Marks et al., 2013; Harder  
777 and Pomeroy, 2013), but accuracy assessment of these techniques themselves are lacking under a  
778 wide range of different conditions.

779

780 A variety of accuracy assessments are needed that will require co-located distributed  
781 measurements. One critical accuracy assessment involves the consistency of different  
782 precipitation phase prediction methods under different climate and atmospheric conditions.  
783 Assessing the effects of climate and atmospheric conditions requires measurements from a  
784 variety of sites covering a range of hydroclimatic conditions and record lengths that span the  
785 conceivable range of atmospheric conditions at a given site. Another important evaluation metric  
786 is the performance over different time steps. Harder and Pomeroy (2013) showed that  
787 hydrometeor and temperature-based prediction methods had errors that substantially decreased  
788 across shorter time steps. Identifying the effects of time step length on the accuracy of different  
789 prediction methods has been relatively unexplored, but is critical to selecting the proper method  
790 for different hydrological applications. Finally, the performance metrics used to assess accuracy  
791 should be carefully considered. The applications of precipitation phase prediction methods are

792 diverse, necessitating a wide variety of performance metrics, including the probability of snow  
793 versus rain (Dai, 2008), the error in annual or total snow/rain accumulation (Rajagopal and  
794 Harpold, 2016), performance under extreme conditions of precipitation amount and intensity,  
795 determination of the snow-rain elevation (Marks et al., 2013), and uncertainty arising from  
796 measurement error and accuracy. Comparison of different metrics across a wide-variety of sites  
797 and conditions is lacking but is greatly needed to advance cold-region hydrologic science.

798

#### 799 5.5 Develop spatially resolved products

800 Many hydrological applications will benefit from gridded data products that are easily integrated  
801 into standard hydrological models. Currently, very few options exist for gridded data  
802 precipitation phase products. Instead, most hydrological models have some type of submodel or  
803 simple scheme that specifies precipitation phase as rain, snow, or mixed (see Section 4). While  
804 testing PPM with ground based observations could lead to improved submodels, we believe  
805 development of gridded forcing data may be an easier and more effective solution for many  
806 hydrological modeling applications.

807

808 Gridded data products could be derived from a combination of remote sensing and existing  
809 model products, but would need to be extensively evaluated. The NASA GPM mission is  
810 beginning to produce gridded precipitation phase products at 3-hour and 0.1 degree resolution.  
811 However, GPM phase is measured at the top of the atmosphere, typically relies on simple  
812 temperature-thresholds, and is yet to be validated with ground based observations. Another  
813 existing product is the Snow Data Assimilation System (SNODAS) that estimates liquid and  
814 solid precipitation at the 1 km scale. However, the developers of SNODAS caution that it is not  
815 suitable for estimating storm totals or regional differences. Furthermore, to our knowledge the  
816 precipitation phase product from SNODAS has not been validated with ground observations. We  
817 suggest the development of new gridded data products that utilize new PPM (i.e. Harder and  
818 Pomeroy, 2013) and new and expanded observational datasets, such as atmospheric information  
819 and radar estimates. We advocate for the development of multiple gridded products that can be  
820 evaluated with ground observations to compare and contrast their strengths. Accurate gridded  
821 phase products rely on the ability to represent the physics of water vapor and energy flows in  
822 complex terrain (e.g. Holden et al., 2010) where statistical downscaling methods are typically

823 insufficient (Gutmann et al., 2012). This would also allow for ensembles of phase estimates to be  
824 used in hydrological models, similar to what is currently being done with gridded precipitation  
825 estimates.

826

## 827 5.6 Characterization of regional variability and response to climate change

828 The inclusion of new datasets, better validation of PPM, and development of gridded data  
829 products will poise the hydrologic community to improve hydrological predictions and better  
830 quantify regional sensitivity of phase change to climate changes. Because broad-scale techniques  
831 applied to assess changes in precipitation phase and snowfall have relied on temperature, both  
832 regionally (Klos et al., 2014; Pierce and Cayan, 2013; Knowles et al., 2006) and globally  
833 (Kapnick and Delworth, 2013; O’Gorman, 2014), they have not fully considered the potential  
834 non-linearities created by the absence of wet bulb depressions and humidity in assessment of  
835 sensitivity to changes in phase. Consequently, the effects of changes from snow to rain from  
836 warming and corresponding changes in humidity will be difficult to predict with the current  
837 PPM. Recent efforts by Rajagopal and Harpold (2016) have demonstrated that simple  
838 temperature thresholds are insufficient to characterize snow-rain transition across the western  
839 U.S. (Figure 3), perhaps because of differences in humidity. An increased focus on future  
840 humidity trends, patterns, and GCM simulation errors (Pierce et al., 2013) and availability of  
841 downscaled humidity products at increasingly finer scales (e.g.: Abatzoglou, 2013; Pierce and  
842 Cayan, 2016) will enable detailed assessments of the relative role of temperature and humidity in  
843 future precipitation phase changes. Recent remote sensing platforms, such as GPM, may offer an  
844 additional tool to assess regional variability, however, the current GPM precipitation phase  
845 product relies on wet bulb temperatures based on model output and not microwave-based  
846 observations (Huffman et al., 2015). Besides issues with either spatial or temporal resolution or  
847 coverage, one of the main challenges in using remotely sensed data for distinguishing between  
848 frozen and liquid hydrometeors is the lack of validation. Where products have been validated, the  
849 results are usually only relevant for the locale of the study area. Spaceborne radar combined with  
850 ground-based radar offers perhaps the most promising solution, but given the non-unique  
851 relationship between radar reflectivity and snowfall, further testing is necessary in order to  
852 develop reliable algorithms.

853

854 Future work is needed to improve projections of changes in snowpack and water availability  
855 from regional to global scales. This local to sub-regional characterization is needed for water  
856 resource prediction and to better inform decision and policy makers. In particular, the ability to  
857 predict the transitional rain-snow elevations and its uncertainty is critical information for a  
858 variety of end-users, including state and municipal water agencies, flood forecasters, agricultural  
859 water boards, transportation agencies, and wildlife, forest, and land managers. Fundamental  
860 advancements in characterizing regional variability are possible by addressing the research  
861 challenges detailed in sections 5.1-5.5.

862

## 863 6. Conclusions

864 Our review paper is a step towards communicating the potential bottlenecks in hydrological  
865 modeling caused by poor representation of precipitation phase (Figure 1). Our goals are to  
866 demonstrate that major research gaps in our ability to PPM are contributing to error and reducing  
867 predictive skill in hydrological modeling. By highlighting the research gaps that could advance  
868 the science of PPM, we provide a roadmap for future advances (Figure 4). While many of the  
869 research gaps are recognized by the community and are being pursued, including incorporating  
870 atmospheric and humidity information, while others remain essentially unexplored (e.g.  
871 production of gridded data, widespread ground validation, and remote sensing validation).

872

873 The key points that must be communicated to the hydrologic community and its funding  
874 agencies can be distilled into the following two statements: 1) current PPM algorithms are too  
875 simple and are not well-validated for most locations, 2) the lack of sophisticated PPM increases  
876 the uncertainty in estimation of hydrological sensitivity to changes in precipitation phase at local  
877 to regional scales. We advocate for better incorporation of new information (5.1-5.2) and  
878 improved validation methods (5.3-5.4) to advance our current PPM methods and observations.  
879 These improved PPM algorithms and remote-sensing observations will be capable of developing  
880 gridded datasets (5.5) and providing new insight that reduce the uncertainty of predicting  
881 regional changes from snow to rain (5.6). A concerted effort by the hydrological and atmospheric  
882 science communities to address the PPM challenge will remedy current limitations in  
883 hydrological modeling of precipitation phase, advance of understanding of cold regions  
884 hydrology, and provide better information to decision makers.

885 Acknowledgements

886 This work was conducted as a part of an Innovation Working Group supported by the Idaho,  
887 Nevada, and New Mexico EPSCoR Programs and by the National Science Foundation under  
888 award numbers IIA-1329469, IIA-1329470 and IIA-1329513. Adrian Harpold was partially  
889 supported by USDA NIFA NEV05293. Adrian Harpold and Rina Schumer were supported by  
890 the NASA EPSCOR Cooperative Agreement #NNX14AN24A. Timothy Link was partially  
891 supported by the Department of the Interior Northwest Climate Science Center (NW CSC)  
892 through a Cooperative Agreement #G14AP00153 from the United States Geological Survey  
893 (USGS). Seshadri Rajagopal was partially supported by research supported by NSF/USDA grant  
894 (#1360506/#1360507) and startup funds provided by Desert Research Institute. The contents of  
895 this manuscript are solely the responsibility of the authors and do not necessarily represent the  
896 views of the NW CSC or the USGS. This manuscript is submitted for publication with the  
897 understanding that the United States Government is authorized to reproduce and distribute  
898 reprints for Governmental purposes.

899 **References:**

- 900 Abatzoglou, J. T.: Development of gridded surface meteorological data for ecological  
901 applications and modelling, *International Journal of Climatology*, 33, 121-131,  
902 10.1002/joc.3413, 2013.
- 903 Anderson, E., 2006, Snow Accumulation and Ablation Model – Snow-17, available online at  
904 [http://www.nws.noaa.gov/oh/hrl/nwsrfs/users\\_manual/part2/\\_pdf/22snow17.pdf](http://www.nws.noaa.gov/oh/hrl/nwsrfs/users_manual/part2/_pdf/22snow17.pdf), accessed August,  
905 2016.
- 906 Arkin, P. A., and Ardanuy, P. E.: Estimating climatic-scale precipitation from space: a review, *J.*  
907 *Climate*, 2, 1229-1238, 1989.
- 908 Arnold, J.G., Kiniry, J.R., Srinivasan R., Williams, J.R, Haney, E.B., and Neitsch S.L., 2012,  
909 SWAT Input/Output Documentation, Texas Water Resources Institute, TR-439, available  
910 online at <http://swat.tamu.edu/media/69296/SWAT-IO-Documentation-2012.pdf>, accessed  
911 August, 2016.
- 912 Bales, R. C., Molotch, N. P., Painter, T. H., Dettinger, M. D., Rice, R., and Dozier, J.: Mountain  
913 hydrology of the western United States, *Water Resources Research*, 42,  
914 10.1029/2005wr004387, 2006.
- 915 Barnett, T. P., Adam, J. C., and Lettenmaier, D. P.: Potential impacts of a warming climate on  
916 water availability in snow-dominated regions, *Nature*, 438, 303-309, 10.1038/nature04141,  
917 2005.
- 918 Battaglia, A., Rustemeier, E., Tokay, A., Blahak, U., and Simmer, C.: PARSIVEL Snow  
919 Observations: A Critical Assessment, *Journal of Atmospheric and Oceanic Technology*, 27,  
920 333-344, 10.1175/2009jtecha1332.1, 2010.
- 921 Berghuijs, W. R., Woods, R. A., and Hrachowitz, M.: A precipitation shift from snow towards  
922 rain leads to a decrease in streamflow, *Nature Climate Change*, 4, 583-586,  
923 10.1038/nclimate2246, 2014.
- 924 Bernauer, F., Hurkamp, K., Ruhm, W., and Tschiersch, J.: Snow event classification with a 2D  
925 video disdrometer - A decision tree approach, *Atmospheric Research*, 172, 186-195, 2016.

926 Bergström, S. 1995. The HBV model. In: Singh, V.P. (Ed.) Computer Models of Watershed  
927 Hydrology. Water Resources Publications, Highlands Ranch, CO., pp. 443-476.

928 Berris, S. N., and Harr, R. D.: Comparative snow accumulation and melt during rainfall in  
929 forested and clear-cut plots in the Western Cascades of Oregon, Water Resources Research,  
930 23, 135-142, 10.1029/WR023i001p00135, 1987.

931 Bicknell, B.R., Imhoff, J.C., Kittle, J.L., Jr., Donigian, A.S., Jr., and Johanson, R.C.,  
932 Hydrological Simulation Program--Fortran, User's manual for version 11: U.S.  
933 Environmental Protection Agency, National Exposure Research Laboratory, Athens, Ga.,  
934 EPA/600/R-97/080, 755 p., 1997.

935 Boe, E. T.: Assessing Local Snow Variability Using a Network of Ultrasonic Snow Depth  
936 Sensors, Master of Science in Hydrologic Sciences, Geosciences, Boise State, 2013.

937 Boodoo, S., Hudak, D., Donaldson, N., and Leduc, M.: Application of Dual-Polarization Radar  
938 Melting-Layer Detection Algorithm, Journal of Applied Meteorology and Climatology, 49,  
939 1779-1793, 10.1175/2010jamc2421.1, 2010.

940 Borrmann, S., and Jaenicke, R.: Application of microholography for ground-based in-situ  
941 measurements in stratus cloud layers - a case study, Journal of Atmospheric and Oceanic  
942 Technology, 10, 277-293, 10.1175/1520-0426(1993)010<0277:aomf>2.0.co;2, 1993.

943 Braun, L. N.: Simulation of snowmelt-runoff in lowland and lower alpine regions of Switzerland,  
944 Diss. Naturwiss. ETH Zürich, Nr. 7684, 0000. Ref.: Ohmura, A.; Korref.: Vischer, D.;  
945 Korref.: Lang, H., 1984.

946 Cao, Q., Hong, Y., Chen, S., Gourley, J. J., Zhang, J., and Kirstetter, P. E.: Snowfall  
947 Detectability of NASA's CloudSat: The First Cross-Investigation of Its 2C-Snow-Profile  
948 Product and National Multi-Sensor Mosaic QPE (NMQ) Snowfall Data, Progress in  
949 Electromagnetics Research-Pier, 148, 55-61, 10.2528/pier14030405, 2014.

950 Cayan, D. R., Kammerdiener, S. A., Dettinger, M. D., Caprio, J. M., and Peterson, D. H.:  
951 Changes in the onset of spring in the western United States, Bulletin of the American  
952 Meteorological Society, 82, 399-415, 10.1175/1520-0477(2001)082<0399:citoos>2.3.co;2,  
953 2001.



954 Chandrasekar, V., Keranen, R., Lim, S., and Moisseev, D.: Recent advances in classification of  
955 observations from dual polarization weather radars, *Atmospheric Research*, 119, 97-111,  
956 10.1016/j.atmosres.2011.08.014, 2013.

957 Chen, S., Gourley, J. J., Hong, Y., Cao, Q., Carr, N., Kirstetter, P.-E., Zhang, J., and Flamig, Z.:  
958 Using citizen science reports to evaluate estimates of surface precipitation type, *Bulletin of*  
959 *the American Meteorological Society*, 10.1175/BAMS-D-13-00247.1, 2015.

960 Dai, A.: Temperature and pressure dependence of the rain-snow phase transition over land and  
961 ocean, *Geophysical Research Letters*, 35, 10.1029/2008gl033295, 2008.

962 Ding, B., Yang, K., Qin, J., Wang, L., Chen, Y., and He, X.: The dependence of precipitation  
963 types on surface elevation and meteorological conditions and its parameterization, *Journal*  
964 *of Hydrology*, 513, 154-163, 10.1016/j.jhydrol.2014.03.038, 2014.

965 Eddington, L. W.: *Satellite-Derived Moisture-Bogusing Profiles for the North Atlantic Ocean*,  
966 DTIC Document, 1989.

967 Elmore, K. L.: The NSSL Hydrometeor Classification Algorithm in Winter Surface  
968 Precipitation: Evaluation and Future Development, *Weather and Forecasting*, 26, 756-765,  
969 10.1175/waf-d-10-05011.1, 2011.

970 Fang, X., Pomeroy, J. W., Ellis, C. R., MacDonald, M. K., DeBeer, C. M., and Brown, T.: Multi-  
971 variable evaluation of hydrological model predictions for a headwater basin in the Canadian  
972 Rocky Mountains, *Hydrol. Earth Syst. Sci.*, 17, 1635-1659, 10.5194/hess-17-1635-2013,  
973 2013.

974 Fatichi, S., Vivoni, E. R., Ogden, F. L., Ivanov, V. Y., Mirus, B., Gochis, D., Downer, C. W.,  
975 Camporese, M., Davison, J. H., Ebel, B., Jones, N., Kim, J., Mascaro, G., Niswonger, R.,  
976 Restrepo, P., Rigon, R., Shen, C., Sulis, M., and Tarboton, D.: An overview of current  
977 applications, challenges, and future trends in distributed process-based models in hydrology,  
978 *Journal of Hydrology*, 537, 45-60, 2016.

979 Feiccabrino, J., Lundberg, A., and Gustafsson, D.: Improving surface-based precipitation phase  
980 determination through air mass boundary identification, *Hydrology Research*, 43, 179-191,  
981 10.2166/nh.2012.060, 2013.

982 Feiccabrino, J., Gustafsson, D., and Lundberg, A.: Surface-based precipitation phase  
983 determination methods in hydrological models, *Hydrology Research*, 44, 44-57, 2015.

984 Floyd, W., and Weiler, M.: Measuring snow accumulation and ablation dynamics during rain-on-  
985 snow events: innovative measurement techniques, *Hydrological Processes*, 22, 4805-4812,  
986 10.1002/hyp.7142, 2008.

987 Fritze, H., Stewart, I. T., and Pebesma, E.: Shifts in Western North American Snowmelt Runoff  
988 Regimes for the Recent Warm Decades, *Journal of Hydrometeorology*, 12, 989-1006,  
989 10.1175/2011jhm1360.1, 2011.

990 Froidurot, S., Zin, I., Hingray, B., and Gautheron, A.: Sensitivity of Precipitation Phase over the  
991 Swiss Alps to Different Meteorological Variables, *Journal of Hydrometeorology*, 15, 685-  
992 696, 10.1175/jhm-d-13-073.1, 2014.

993 Garvelmann, J., Pohl, S., and Weiler, M.: From observation to the quantification of snow  
994 processes with a time-lapse camera network, *Hydrology and Earth System Sciences*, 17,  
995 1415-1429, 10.5194/hess-17-1415-2013, 2013.

996 Giangrande, S. E., Krause, J. M., and Ryzhkov, A. V.: Automatic designation of the melting  
997 layer with a polarimetric prototype of the WSR-88D radar, *Journal of Applied Meteorology*  
998 and *Climatology*, 47, 1354-1364, 10.1175/2007jamc1634.1, 2008.

999 Gilmore, M. S., Straka, J. M., and Rasmussen, E. N.: Precipitation Uncertainty Due to Variations  
1000 in Precipitation Particle Parameters within a Simple Microphysics Scheme, *Monthly*  
1001 *Weather Review*, 132, 2610-2627, 10.1175/MWR2810.1, 2004.

1002 Godsey, S. E., Kirchner, J. W., and Tague, C. L.: Effects of changes in winter snowpacks on  
1003 summer low flows: case studies in the Sierra Nevada, California, USA, *Hydrological*  
1004 *Processes*, 28, 5048-5064, 10.1002/hyp.9943, 2014.

1005 Grazioli, J., Tuia, D., and Berne, A.: Hydrometeor classification from polarimetric radar  
1006 measurements: a clustering approach, *Atmospheric Measurement Techniques*, 8, 149-170,  
1007 10.5194/amt-8-149-2015, 2015.

1008 Gusev, E.M. and Nasonova, O.N., Parameterization of Heat and Water Exchange on Land  
1009 Surface for Coupling Hydrologic and Climate Models, *Water Resources.*, 25(4): 421-431,  
1010 1998.

1011 Gutmann, E.D., Rasmussen, R.M., Liu, C., Ikeda, K., Gochis, D., Clark, P.P., Dudhia, J., and  
1012 Gregory, T.: A comparison of statistical and dynamical downscaling of winter precipitation  
1013 over complex terrain, *Journal of Climate*, 25(1): 262-281, 2012.

1014 Harder, P., and Pomeroy, J.: Estimating precipitation phase using a psychrometric energy  
1015 balance method, *Hydrological Processes*, 27, 1901-1914, 10.1002/hyp.9799, 2013.

1016 Harder, P., and Pomeroy, J. W.: Hydrological model uncertainty due to precipitation-phase  
1017 partitioning methods, *Hydrological Processes*, 28, 4311-4327, 2014.

1018 Hauser, D., Amayenc, P., and Nutten, B.: A new optical instrument for simultaneous  
1019 measurement of raindrop diameter and fall speed distributions, *Atmos. Oceanic Technol.*, 1,  
1020 256-259, 1984.

1021 HEC-1, 1998, Flood Hydrograph Package, User's Manual, CPD-1A, Version 4.1, available  
1022 online at, [http://www.hec.usace.army.mil/publications/ComputerProgramDocumentation/HEC-](http://www.hec.usace.army.mil/publications/ComputerProgramDocumentation/HEC-1_UsersManual_(CPD-1a).pdf)  
1023 [1\\_UsersManual\\_\(CPD-1a\).pdf](http://www.hec.usace.army.mil/publications/ComputerProgramDocumentation/HEC-1_UsersManual_(CPD-1a).pdf), accessed August, 2016.

1024 Hedrick, A. R., and Marshall, H.-P.: Automated Snow Depth Measurements in Avalanche  
1025 Terrain Using Time-Lapse Photography, 2014 International Snow Science Workshop, 2014,

1026 Holden, Z. A., Abatzoglou, J. T., Luce, C. H., & Baggett, L. S. Empirical downscaling of daily  
1027 minimum air temperature at very fine resolutions in complex terrain. *Agricultural and*  
1028 *Forest Meteorology*, 151, 1066-1073. doi:10.1016/j.agrformet.2011.03.011, 2011.

1029 Hou, A. Y., Kakar, R. K., Neeck, S., Azarbarzin, A. A., Kummerow, C. D., Kojima, M., Oki, R.,  
1030 Nakamura, K., and Iguchi, T.: The global precipitation measurement mission, *Bulletin of the*  
1031 *American Meteorological Society*, 95, 701-722, 2014.

1032 Isaac, G. A., Joe, P. I., Mailhot, J., Bailey, M., Bélair, S., Boudala, F. S., . . . Wilson, L. J.  
1033 Science of nowcasting Olympic weather for Vancouver 2010 (SNOW-V10): A World  
1034 Weather Research Programme project. *Pure and Applied Geophysics*, 171(1-2), 1-24.  
1035 doi:10.1007/s00024-012-0579-0, 2014.

1036 Jepsen, S. M., Harmon, T. C., Meadows, M. W., and Hunsaker, C. T.: Hydrogeologic influence  
1037 on changes in snowmelt runoff with climate warming: Numerical experiments on a mid-  
1038 elevation catchment in the Sierra Nevada, USA, *Journal of Hydrology*, 533, 332-342,  
1039 10.1016/j.jhydrol.2015.12.010, 2016.

1040 Joe, P., Scott, B., Doyle, C., Isaac, G., Gultepe, I., Forsyth, D., . . . Boudala, F. The monitoring  
1041 network of the Vancouver 2010 Olympics. *Pure and Applied Geophysics*, 171(1-2), 25-58,  
1042 doi:10.1007/s00024-012-0588-z, 2014.

1043 Joss, J., and Waldvogel, A.: Ein Spektograph fuer Niederschlagstropfen mit automatischer  
1044 Auswertung, *Pure Appl. Geophys*, 68, 240--246, 1967.

1045 Kalnay, E., and Cai, M.: Impact of urbanization and land-use change on climate, *Nature*, 423,  
1046 528-531, 10.1038/nature01675, 2003.

1047 Kaplan, M. L., Vellore, R. K., Marzette, P. J., and Lewis, J. M.: The role of windward-side  
1048 diabatic heating in Sierra Nevada spillover precipitation, *Journal of Hydrometeorology*, 13,  
1049 1172-1194, 2012.

1050 Kapnick, S. B. and Delworth, T. L.: Controls of global snow under a changed climate, *Journal of*  
1051 *Climate*, 26, 5537-5562, 2013.

1052 Kidd, C.: On rainfall retrieval using polarization-corrected temperatures, *International Journal of*  
1053 *Remote Sensing*, 19, 981-996, 10.1080/014311698215829, 1998.

1054 Kidd, C., and Huffman, G.: Global precipitation measurement, *Meteorological Applications*, 18,  
1055 334-353, 10.1002/met.284, 2011.

1056 Kienzle, S. W.: A new temperature based method to separate rain and snow, *Hydrological*  
1057 *Processes*, 22, 5067-5085, 10.1002/hyp.7131, 2008.

1058 Kim, M. J., Weinman, J. A., Olson, W. S., Chang, D. E., Skofronick-Jackson, G., and Wang, J.  
1059 R.: A physical model to estimate snowfall over land using AMSU-B observations, *Journal*  
1060 *of Geophysical Research-Atmospheres*, 113, 16, 10.1029/2007jd008589, 2008.

1061 Kirchner, J. W.: Getting the right answers for the right reasons: Linking measurements, analyses,  
1062 and models to advance the science of hydrology, *Water Resources Research*, 42,  
1063 10.1029/2005wr004362, 2006.

1064 Kite, G. 1995. The HBV model. In: Singh, V.P. (Ed.) *Computer Models of Watershed*  
1065 *Hydrology*. Water Resources Publications, Highlands Ranch, CO., pp. 443-476.

1066 Klos, P. Z., Link, T. E., and Abatzoglou, J. T.: Extent of the rain-snow transition zone in the  
1067 western US under historic and projected climate, *Geophysical Research Letters*, 41, 4560-  
1068 4568, 10.1002/2014gl060500, 2014.

1069 Knollenberg, R. G.: Some results of measurements of latent heat released from seeded stratus,  
1070 *Bulletin of the American Meteorological Society*, 51, 580-&, 1970.

1071 Knowles, N., Dettinger, M. D., and Cayan, D. R.: Trends in snowfall versus rainfall in the  
1072 Western United States, *Journal of Climate*, 19, 4545-4559, 2006.

1073 Kongoli, C., Pellegrino, P., Ferraro, R. R., Grody, N. C., and Meng, H.: A new snowfall  
1074 detection algorithm over land using measurements from the Advanced Microwave Sounding  
1075 Unit (AMSU), *Geophysical Research Letters*, 30, 10.1029/2003gl017177, 2003.

1076 Kongoli, C., Meng, H., Dong, J., and Ferraro, R.: A snowfall detection algorithm over land  
1077 utilizing high-frequency passive microwave measurements-Application to ATMS, *Journal*  
1078 *of Geophysical Research-Atmospheres*, 120, 1918-1932, 10.1002/2014jd022427, 2015.

1079 Kruger, A., and Krajewski, W. F.: Two-dimensional video disdrometer: A description, *Journal of*  
1080 *Atmospheric and Oceanic Technology*, 19, 602-617, 10.1175/1520-  
1081 0426(2002)019<0602:tdvdad>2.0.co;2, 2002.

1082 Kulie, M. S., Milani, L., Wood, N. B., Tushaus, S. A., Bennartz, R., and L'Ecuyer, T. S.: A  
1083 Shallow Cumuliform Snowfall Census Using Spaceborne Radar, *Journal of*  
1084 *Hydrometeorology*, 17, 1261-1279, 10.1175/jhm-d-15-0123.1, 2016.

1085 L'hôte, Y., Chevallier, P., Coudrain, A., Lejeune, Y., and Etchevers, P.: Relationship between  
1086 precipitation phase and air temperature: comparison between the Bolivian Andes and the  
1087 Swiss Alps/Relation entre phase de précipitation et température de l'air: comparaison entre  
1088 les Andes Boliviennes et les Alpes Suisses, *Hydrological sciences journal*, 50, 2005.

1089 Leavesley, G. H., Restrepo, P. J., Markstrom, S. L., Dixon, M., and Stannard, L. G.: The  
1090 Modular Modeling System (MMS): User's Manual, U.S. Geological Survey, Denver,  
1091 COOpen File Report 96-151, 1996.

1092 Lempio, G. E., Bumke, K., and Macke, A.: Measurement of solid precipitation with an optical  
1093 disdrometer, *Advances in Geosciences*, 10, 91-97, 2007.

1094 Lewis, J., Lakshmiarahan, S., and Dhall, S.: Dynamic Data Assimilation: A Least Squares  
1095 Approach, Cambridge Univ. Press, 745 pp., 2006.

1096 Lin, Y.-L.: Mesoscale Dynamics, Cambridge University Press, 630 pp., 2007.

1097 Liu, G.: Deriving snow cloud characteristics from CloudSat observations, Journal of Geophysical  
1098 Research-Atmospheres, 113, 10.1029/2007jd009766, 2008.

1099 Loffler-Mang, M., Kunz, M., and Schmid, W.: On the performance of a low-cost K-band  
1100 Doppler radar for quantitative rain measurements, Journal of Atmospheric and Oceanic  
1101 Technology, 16, 379-387, 10.1175/1520-0426(1999)016<0379:otpoal>2.0.co;2, 1999.

1102 Luce, C. H., and Holden, Z. A.: Declining annual streamflow distributions in the Pacific  
1103 Northwest United States, 1948-2006, Geophysical Research Letters, 36,  
1104 10.1029/2009gl039407, 2009.

1105 Lundquist, J. D., Neiman, P. J., Martner, B., White, A. B., Gottas, D. J., and Ralph, F. M.: Rain  
1106 versus snow in the Sierra Nevada, California: Comparing Doppler profiling radar and  
1107 surface observations of melting level, Journal of Hydrometeorology, 9, 194-211,  
1108 10.1175/2007jhm853.1, 2008.

1109 Lynch-Stieglitz, M.: The development and validation of a simple snow model for the GISS  
1110 GCM, Journal of Climate, 7, 1842-1855, 1994.

1111 Marks, D., Link, T., Winstral, A., and Garen, D.: Simulating snowmelt processes during rain-on-  
1112 snow over a semi-arid mountain basin, Annals of Glaciology, 32, 195-202, 2001.

1113 Marks, D., Winstral, A., Reba, M., Pomeroy, J., and Kumar, M.: An evaluation of methods for  
1114 determining during-storm precipitation phase and the rain/snow transition elevation at the  
1115 surface in a mountain basin, Advances in Water Resources, 55, 98-110,  
1116 <http://dx.doi.org/10.1016/j.advwatres.2012.11.012>, 2013.

1117 Martinec, J., and Rango, A.: Parameter values for snowmelt runoff modelling, Journal of  
1118 Hydrology, 84, 197-219, [http://dx.doi.org/10.1016/0022-1694\(86\)90123-X](http://dx.doi.org/10.1016/0022-1694(86)90123-X), 1986.

1119 Martinec J., Rango A., Roberts R., 2008, Snowmelt Runoff Model, User's Manual, available  
1120 online at [http://aces.nmsu.edu/pubs/research/weather\\_climate/SRMSpecRep100.pdf](http://aces.nmsu.edu/pubs/research/weather_climate/SRMSpecRep100.pdf), accessed  
1121 August, 2016.

1122 Matrosov, S. Y., Shupe, M. D., and Djalalova, I. V.: Snowfall retrievals using millimeter-  
1123 wavelength cloud radars, *Journal of Applied Meteorology and Climatology*, 47, 769-777,  
1124 10.1175/2007jamc1768.1, 2008.

1125 Maurer, E. P., and Mass, C.: Using radar data to partition precipitation into rain and snow in a  
1126 hydrologic model, *Journal of Hydrologic Engineering*, 11, 214-221, 10.1061/(asce)1084-  
1127 0699(2006)11:3(214), 2006.

1128 McCabe, G. J., and Wolock, D. M.: General-circulation-model simulations of future snowpack in  
1129 the western United States I. *JAWRA Journal of the American Water Resources Association*,  
1130 35(6), 1473-1484, 1999a.

1131 McCabe, G. J. and Wolock, D. M.: Recent Declines in Western U.S. Snowpack in the Context of  
1132 Twentieth-Century Climate Variability, *Earth Interactions*, 13, 1-15, DOI:  
1133 10.1175/2009EI283.1, 1999b.

1134 McCabe, G. J., Clark, M. P., and Hay, L. E.: Rain-on-snow events in the western United States,  
1135 *Bulletin of the American Meteorological Society*, 88, 319-+, 10.1175/bams-88-3-319, 2007.

1136 McCabe, G. J., and Wolock, D. M.: Long-term variability in Northern Hemisphere snow cover  
1137 and associations with warmer winters, *Climatic Change*, 99, 141-153, 2010.

1138 MIKE-SHE User Manual, available online at  
1139 [ftp://ftp.cgs.si/Uporabniki/UrosZ/mike/Manuals/MIKE\\_SHE/MIKE\\_SHE.htm](ftp://ftp.cgs.si/Uporabniki/UrosZ/mike/Manuals/MIKE_SHE/MIKE_SHE.htm), accessed August,  
1140 2016.

1141 Milly, P. C. D., Betancourt, J., Falkenmark, M., Hirsch, R. M., Kundzewicz, Z. W., Lettenmaier,  
1142 D. P., and Stouffer, R. J.: Climate change - Stationarity is dead: Whither water  
1143 management?, *Science*, 319, 573-574, 10.1126/science.1151915, 2008.

1144 Minder, J. R.: The Sensitivity of Mountain Snowpack Accumulation to Climate Warming,  
1145 *Journal of Climate*, 23, 2634-2650, 10.1175/2009jcli3263.1, 2010.

1146 Minder, J. R., and Kingsmill, D. E.: Mesoscale Variations of the Atmospheric Snow Line over  
1147 the Northern Sierra Nevada: Multiyear Statistics, Case Study, and Mechanisms, *Journal of*  
1148 *the Atmospheric Sciences*, 70, 916-938, 10.1175/jas-d-12-0194.1, 2013.

1149 Mitchell K., Ek, M., Wong, V., Lohmann, D., Koren, V., Schaake, J., Duan, Q., Gayno, G.,  
1150 Moore, B., Grunmann, P., Tarpley, D., Ramsay, B., Chen, F., Kim, J., Pan, H.L., Lin, Y.,  
1151 Marshall, C., Mahrt, L., Meyers, T., and Ruscher, P.: 2005, Noah Land-Surface Model,  
1152 User's Guide, version 2.7.1, available at  
1153 [ftp://ftp.emc.ncep.noaa.gov/mmb/gcp/ldas/noahls/ver\\_2.7.1](ftp://ftp.emc.ncep.noaa.gov/mmb/gcp/ldas/noahls/ver_2.7.1), accessed August, 2016.

1154 Mizukami, N., Koren, V., Smith, M., Kingsmill, D., Zhang, Z. Y., Cosgrove, B., and Cui, Z. T.:  
1155 The Impact of Precipitation Type Discrimination on Hydrologic Simulation: Rain-Snow  
1156 Partitioning Derived from HMT-West Radar-Detected Brightband Height versus Surface  
1157 Temperature Data, *Journal of Hydrometeorology*, 14, 1139-1158, 10.1175/jhm-d-12-035.1,  
1158 2013.

1159 Morrison, H., Curry, J., and Khvorostyanov, V.: A new double-moment microphysics  
1160 parameterization for application in cloud and climate models. Part I: Description, *Journal of*  
1161 *the Atmospheric Sciences*, 62, 1665-1677, 2005.

1162 Motoyama, H.: Simulation of seasonal snowcover based on air temperature and precipitation,  
1163 *Journal of Applied Meteorology*, 29, 1104-1110, 1990.

1164 Newman, A. J., Kucera, P. A., & Bliven, L. F.. Presenting the snowflake video imager (SVI).  
1165 *Journal of Atmospheric and Oceanic Technology*, 26(2), 167-179, 2009.  
1166 doi:10.1175/2008jtecha1148.1

1167 NOAA, 2016. NEXRAD Data Archive, Inventory and Access, available online at  
1168 <https://www.ncdc.noaa.gov/nexradinv/> accessed 11/10/2016

1169 Noh, Y. J., Liu, G. S., Jones, A. S., and Haar, T. H. V.: Toward snowfall retrieval over land by  
1170 combining satellite and in situ measurements, *Journal of Geophysical Research-*  
1171 *Atmospheres*, 114, 10.1029/2009jd012307, 2009.

1172 O’Gorman, P.A.: Contrasting responses of mean and extreme snowfall to climate change,  
1173 *Nature*, 512, 416-418, 2014.

1174 Olsen, A.: Snow or rain?—A matter of wet-bulb temperature, thesis, Uppsala Univ., Uppsala,  
1175 Sweden.(Available at [http://www. geo. uu. se/luva/exarb/2003/Arvid\\_ Olsen. pdf](http://www.geo.uu.se/luva/exarb/2003/Arvid_Olsen.pdf)), 2003.



1176 Olson, W. S., Kummerow, C. D., Heymsfield, G. M., and Giglio, L.: A method for combined  
1177 passive-active microwave retrievals of cloud and precipitation profiles, *Journal of Applied*  
1178 *Meteorology*, 35, 1763-1789, 10.1175/1520-0450(1996)035<1763:amfcpm>2.0.co;2, 1996.

1179 Pachauri, R. K.: Intergovernmental panel on climate change (IPCC): Keynote address,  
1180 *Environmental Science and Pollution Research*, 9, 436-438, 2002.

1181 Pagano, T. C., Wood, A. W., Ramos, M. H., Cloke, H. L., Pappenberger, F., Clark, M. P.,  
1182 Cranston, M., Kavetski, D., Mathevet, T., Sorooshian, S., and Verkade, J. S.: Challenges of  
1183 Operational River Forecasting, *Journal of Hydrometeorology*, 15, 1692-1707, 10.1175/jhm-  
1184 d-13-0188.1, 2014.

1185 Parajka, J., Haas, P., Kirnbauer, R., Jansa, J., and Bloeschl, G.: Potential of time-lapse  
1186 photography of snow for hydrological purposes at the small catchment scale, *Hydrological*  
1187 *Processes*, 26, 3327-3337, 10.1002/hyp.8389, 2012.

1188 Park, H., Ryzhkov, A. V., Zrnica, D. S., and Kim, K.-E.: The Hydrometeor Classification  
1189 Algorithm for the Polarimetric WSR-88D: Description and Application to an MCS, *Weather*  
1190 *and Forecasting*, 24, 730-748, 10.1175/2008waf2222205.1, 2009.

1191 Pierce, D. W. and Cayan, D. R.: The uneven response of different snow measures to human-  
1192 induced climate warming. *Journal of Climate*, 26, 4148-4167, 2013.

1193 Pierce, D. W., Westerling, A. L., & Oyler, J.. Future humidity trends over the western united  
1194 states in the CMIP5 global climate models and variable infiltration capacity hydrological  
1195 modeling system. *Hydrology and Earth System Sciences*, 17(5), 1833-1850, 2013.

1196 Pierce, D. W. and Cayan, D. R. Downscaling humidity with localized constructed analogs  
1197 (LOCA) over the conterminous united states. *Climate Dynamics*, 47, 411-431, 2016.

1198 Pipes, A., and Quick, M. C.: UBC watershed model users guide, Department of Civil  
1199 Engineering, University of British Columbia, 1977.

1200 Rajagopal, S., and Harpold, A.: Testing and Improving Temperature Thresholds for Snow and  
1201 Rain Prediction in the Western United States, *Journal of American Water Resources*  
1202 *Association*, 2016.

1203 Rasmussen, R., Baker, B., Kochendorfer, J., Meyers, T., Landolt, S., Fischer, A. P., Black, J.,  
1204 Thériault, J. M., Kucera, P., Gochis, D., Smith, C., Nitu, R., Hall, M., Ikeda, K., and  
1205 Gutmann, E.: How Well Are We Measuring Snow: The NOAA/FAA/NCAR Winter  
1206 Precipitation Test Bed, *Bulletin of the American Meteorological Society*, 93, 811-829,  
1207 10.1175/BAMS-D-11-00052.1, 2012.

1208 Reisner, J., Rasmussen, R. M., and Bruintjes, R.: Explicit forecasting of supercooled liquid water  
1209 in winter storms using the MM5 mesoscale model, *Quarterly Journal of the Royal*  
1210 *Meteorological Society*, 124, 1071-1107, 1998.

1211 Rojas, R., Feyen, L., Dosio, A., and Bavera, D.: Improving pan-European hydrological  
1212 simulation of extreme events through statistical bias correction of RCM-driven  
1213 climate simulations, *Hydrology and Earth System Sciences*, 15, 2599, 2011.

1214 Safeeq, M., Mauger, G. S., Grant, G. E., Arismendi, I., Hamlet, A. F., and Lee, S. Y.: Comparing  
1215 Large-Scale Hydrological Model Predictions with Observed Streamflow in the Pacific  
1216 Northwest: Effects of Climate and Groundwater, *Journal of Hydrometeorology*, 15, 2501-  
1217 2521, 10.1175/jhm-d-13-0198.1, 2014.

1218 Sevruk, B.: Assessment of snowfall proportion in monthly precipitation in Switzerland, *Zbornik*  
1219 *meteoroloskih i Hidroloskih Radovav Beograd*, 10, 315-318, 1984.

1220 Shamir, E., and Georgakakos, K. P.: Distributed snow accumulation and ablation modeling in the  
1221 American River basin, *Advances in Water Resources*, 29, 558-570,  
1222 10.1016/j.advwatres.2005.06.010, 2006.

1223 Skamarock, W. C., Klemp, J. B., Dudhia, J., Gill, D. O., Barker, D. M., Duda, M. G., Huang, X.-  
1224 Y., Wang, W., and Powers, J. G.: A description of the advanced research WRF version  
1225 3NCAR Tech. Note NCAR/TN-475+STR, 113, 2008.

1226 Skofronick-Jackson, G., Hudak, D., Petersen, W., Nesbitt, S. W., Chandrasekar, V., Durden, S.,  
1227 Gleicher, K. J., Huang, G.-J., Joe, P., Kollias, P., Reed, K. A., Schwaller, M. R., Stewart, R.,  
1228 Tanelli, S., Tokay, A., Wang, J. R., and Wolde, M.: Global Precipitation Measurement Cold  
1229 Season Precipitation Experiment (GCPEX): For Measurement's Sake, Let It Snow, *Bulletin*  
1230 *of the American Meteorological Society*, 96, 1719-1741, doi:10.1175/BAMS-D-13-00262.1,  
1231 2015.

1232 SNTHERM Online Documentation, available at  
1233 <http://www.geo.utexas.edu/climate/Research/SNOWMIP/SUPERSNOW2/rjordan.html>, accessed  
1234 August, 2016.

1235 Stewart, R. E.: Precipitation Types in the Transition Region of Winter Storms, Bulletin of the  
1236 American Meteorological Society, 73, 287-296, 10.1175/1520-  
1237 0477(1992)073<0287:PTITTR>2.0.CO;2, 1992.

1238 Stewart, R. E., Theriault, J. M., and Henson, W.: On the Characteristics of and Processes  
1239 Producing Winter Precipitation Types near 0 degrees C, Bulletin of the American  
1240 Meteorological Society, 96, 623-639, 10.1175/bams-d-14-00032.1, 2015.

1241 Tague, C.L, and Band, L.E.: RHESSys: Regional Hydro-Ecologic Simulation System—An  
1242 Object Oriented Approach to Spatially Distributed Modeling of Carbon, Water, and Nutrient  
1243 Cycling, Earth Interactions, 8, 19, 1-42, 2004.

1244 Tarboton, D.G., and Luce, C.H., 1996, Utah Energy Balance Snow Accumulation and Melt  
1245 Model (UEB), available online at  
1246 [http://www.fs.fed.us/rm/boise/publications/watershed/rmrs\\_1996\\_tarbotond001.pdf](http://www.fs.fed.us/rm/boise/publications/watershed/rmrs_1996_tarbotond001.pdf), accessed  
1247 August, 2016.

1248 Tarboton, D., Jackson, T., Liu, J., Neale, C., Cooley, K., and McDonnell, J.: A Grid Based  
1249 Distributed Hydrologic Model: Testing Against Data from Reynolds Creek Experimental  
1250 Watershed, Preprints AMS Conf. on Hydrol, 79-84, 1995.

1251 Theriault, J. M., and Stewart, R. E.: On the effects of vertical air velocity on winter precipitation  
1252 types, Natural Hazards and Earth System Sciences, 7, 231-242, 2007.

1253 Theriault, J. M., and Stewart, R. E.: A Parameterization of the Microphysical Processes Forming  
1254 Many Types of Winter Precipitation, Journal of the Atmospheric Sciences, 67, 1492-1508,  
1255 10.1175/2009jas3224.1, 2010.

1256 Theriault, J. M., Stewart, R. E., and Henson, W.: On the Dependence of Winter Precipitation  
1257 Types on Temperature, Precipitation Rate, and Associated Features, Journal of Applied  
1258 Meteorology and Climatology, 49, 1429-1442, 10.1175/2010jamc2321.1, 2010.

1259 Theriault, J. M., Stewart, R. E., and Henson, W.: Impacts of terminal velocity on the trajectory of  
1260 winter precipitation types, *Atmospheric Research*, 116, 116-129,  
1261 10.1016/j.atmosres.2012.03.008, 2012.

1262 Thompson, E. J., Rutledge, S. A., Dolan, B., Chandrasekar, V., and Cheong, B. L.: A Dual-  
1263 Polarization Radar Hydrometeor Classification Algorithm for Winter Precipitation, *Journal*  
1264 *of Atmospheric and Oceanic Technology*, 31, 1457-1481, 10.1175/jtech-d-13-00119.1,  
1265 2014.

1266 Thompson, G., Rasmussen, R. M., and Manning, K.: Explicit forecasts of winter precipitation  
1267 using an improved bulk microphysics scheme. Part I: Description and sensitivity analysis,  
1268 *Monthly Weather Review*, 132, 519-542, 2004.

1269 Thompson, G., Field, P. R., Rasmussen, R. M., and Hall, W. D.: Explicit forecasts of winter  
1270 precipitation using an improved bulk microphysics scheme. Part II: Implementation of a  
1271 new snow parameterization, *Monthly Weather Review*, 136, 5095-5115, 2008.

1272 Todini, E.: The ARNO Rainfall-runoff model, *Journal of Hydrology*, 175, 339-382, 1996.

1273 Tung, C.-P., and Haith, D. A.: Global-warming effects on New York streamflows, *Journal of*  
1274 *Water Resources Planning and Management*, 121, 216-225, 1995.

1275 U.S. Army Corps of Engineers: Summary Report of the Snow Investigation Hydrological  
1276 Practices, 3rd Edition, Chapter 2, 54-56, North Pacific Division, Portland, Oregon, 1956.

1277 Versegny, D., 2009, CLASS-The Canadian Land Surface Scheme, Version 3.4, Technical  
1278 Documentation, Version 1.1, Environment Canada, available online at  
1279 [http://www.usask.ca/ip3/download/CLASS\\_v3\\_4\\_Documentation\\_v1\\_1.pdf](http://www.usask.ca/ip3/download/CLASS_v3_4_Documentation_v1_1.pdf), accessed  
1280 August, 2016.

1281 VIC Documentation, available online at <https://vic.readthedocs.io/en/develop/>, accessed August,  
1282 2016.

1283 Wang, R., Kumar, M., and Marks, D. Anomalous trend in soil evaporation in a semi-arid, snow-  
1284 dominated watershed. *Advances in Water Resources*, 57, 32-40, 2013.

1285 Wang, R., Kumar, M., and Link, T. E.: Potential trends in snowmelt generated peak streamflows  
1286 in a warming climate, *Geophys. Res. Lett.* 43, 10.1002/ 2016GL068935, 2016.

- 1287 Wen, L., Nagabhatla, N., Lu, S., and Wang, S.-Y.: Impact of rain snow threshold temperature on  
1288 snow depth simulation in land surface and regional atmospheric models, *Advances in*  
1289 *Atmospheric Sciences*, 30, 1449-1460, 10.1007/s00376-012-2192-7, 2013.
- 1290 White, A. B., Gattas, D. J., Strem, E. T., Ralph, F. M., and Neiman, P. J.: An automated  
1291 brightband height detection algorithm for use with Doppler radar spectral moments, *Journal*  
1292 *of Atmospheric and Oceanic Technology*, 19, 687-697, 10.1175/1520-  
1293 0426(2002)019<0687:aabhda>2.0.co;2, 2002.
- 1294 White, A. B., Gattas, D. J., Henkel, A. F., Neiman, P. J., Ralph, F. M., and Gutman, S. I.:  
1295 Developing a Performance Measure for Snow-Level Forecasts, *Journal of*  
1296 *Hydrometeorology*, 11, 739-753, 10.1175/2009jhm1181.1, 2010.
- 1297 Whiteman, C. D., Bian, X., & Zhong, S.. Wintertime evolution of the temperature inversion in  
1298 the colorado plateau basin. *Journal of Applied Meteorology*, 38(8), 1103-1117, 1999.
- 1299 Wigmosta, M.S., Vail, L.W., and Lettenmaier, D.P.: A distributed hydrology-vegetation model  
1300 for complex terrain, *Water Resources Research*, 30(6), 1665-1679, 1994.
- 1301 Wilheit, T. T., Chang, A. T. C., King, J. L., Rodgers, E. B., Nieman, R. A., Krupp, B. M.,  
1302 Milman, A. S., Stratigos, J. S., and Siddalingaiah, H.: Microwave radiometric observation  
1303 near 19.35, 92 and 183 GHz of precipitation in tropical storm Cora, *Journal of Applied*  
1304 *Meteorology*, 21, 1137-1145, 10.1175/1520-0450(1982)021<1137:mronag>2.0.co;2, 1982.
- 1305 Wood, A. W., Leung, L. R., Sridhar, V., and Lettenmaier, D.: Hydrologic implications of  
1306 dynamical and statistical approaches to downscaling climate model outputs, *Climatic*  
1307 *change*, 62, 189-216, 2004.
- 1308 Wood, N., L'Ecuyer, T. S., Vane, D., Stephens, G., and Partain, P.: Level 2C snow profile  
1309 process description and interface control document, 2013.
- 1310 Yamazaki, T.: A One-dimensional Land Surface Model Adaptable to Intensely Cold Regions and  
1311 its Applications in Eastern Siberia, 79, 1107-1118, 2001.
- 1312 Yang Z.L., Dickinson, R.E., Robock, A. and Vinniko, K.Y.: Validation of the Snow Submodel of  
1313 the Biosphere–Atmosphere Transfer Scheme with Russian Snow Cover and Meteorological  
1314 Observational Data, *J. Climate*, 10, 353–373, doi: 10.1175/1520-  
1315 0442(1997)010<0353:VOTSSO>2.0.CO;2, 1997.

1316 Yarnell, S. M., Viers, J. H., and Mount, J. F.: Ecology and Management of the Spring Snowmelt  
1317       Recession, *Bioscience*, 60, 114-127, 10.1525/bio.2010.60.2.6, 2010.

1318 Ye, H., Cohen, J., and Rawlins, M.: Discrimination of Solid from Liquid Precipitation over  
1319       Northern Eurasia Using Surface Atmospheric Conditions, *Journal of Hydrometeorology*, 14,  
1320       1345-1355, 10.1175/jhm-d-12-0164.1, 2013.

1321 Yucel, I., Onen, A., Yilmaz, K. K., and Gochis, D. J.: Calibration and evaluation of a flood  
1322       forecasting system: Utility of numerical weather prediction model, data assimilate, and  
1323       satellite-based rainfall, *Journal of Hydrology*, 523, 49-66, 10.1016/j.hydro.2015.01.042,  
1324       2015.

1325 Zängl, G.: Interaction between dynamics and cloud microphysics in orographic precipitation  
1326       enhancement: A high-resolution modeling study of two North Alpine heavy-precipitation  
1327       events, *Monthly weather review*, 135, 2817-2840, 2007.

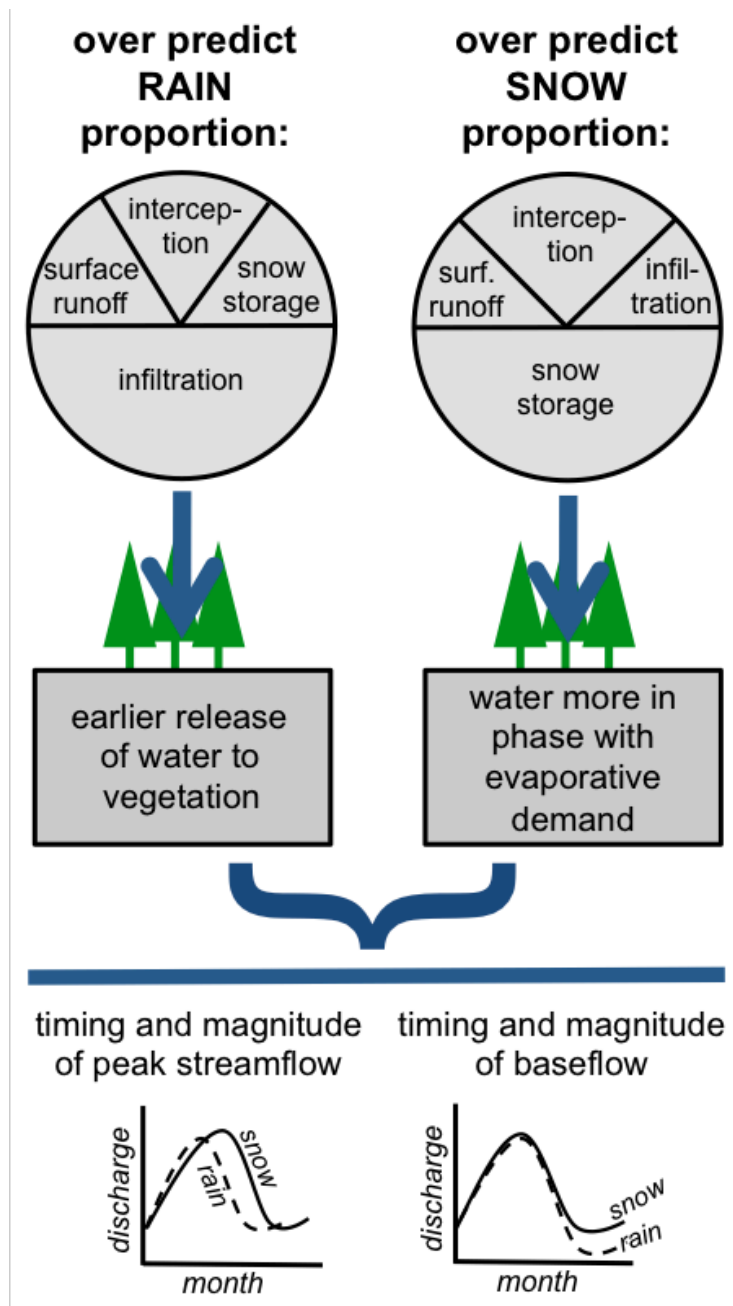
1328 Zanotti, F., Endrizzi, S., Bertoldi, G. and Rigon, R.: The GEOTOP snow module, *Hydrological*  
1329       Processes, 18, 3667–3679. doi:10.1002/hyp.5794, 2004.

1330

1331

1332

1333



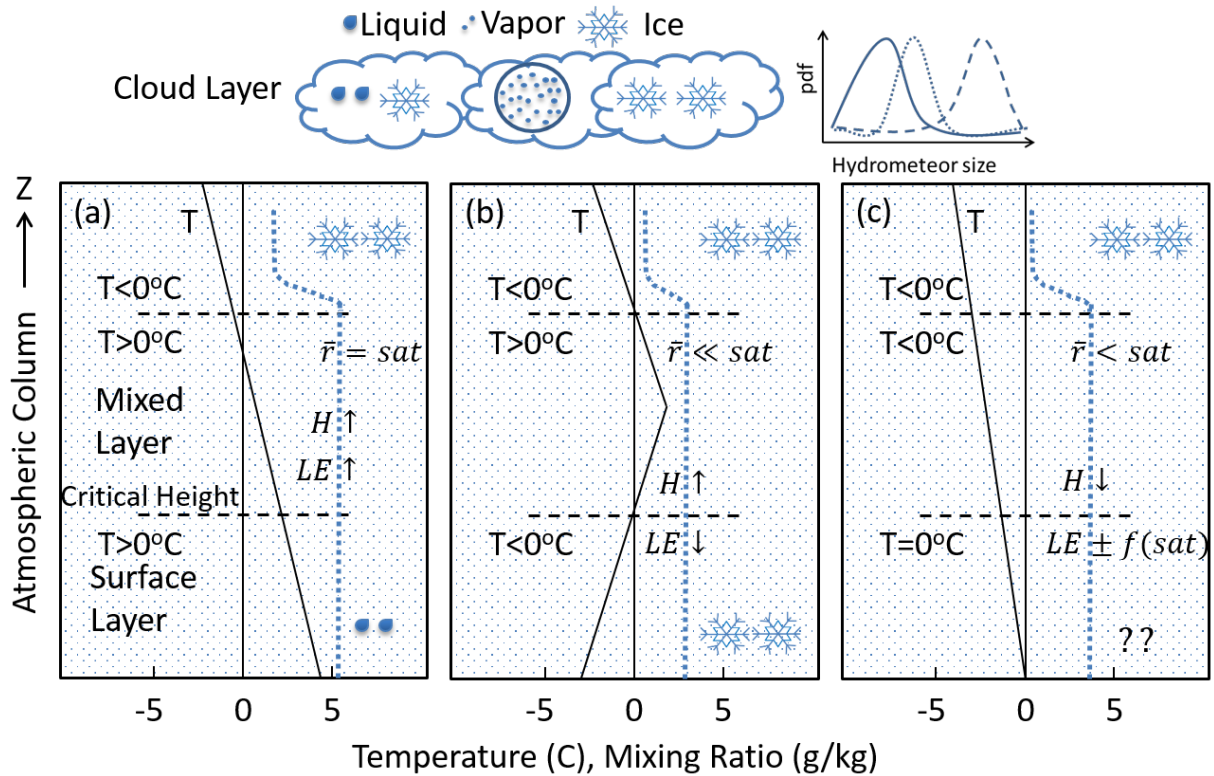
1334

1335 Figure 1: Precipitation phase has numerous implications for modeling the magnitude, storage,

1336 partitioning, and timing of water inputs and outputs. Potentially affecting important

1337 ecohydrological and streamflow quantities important for prediction.

1338



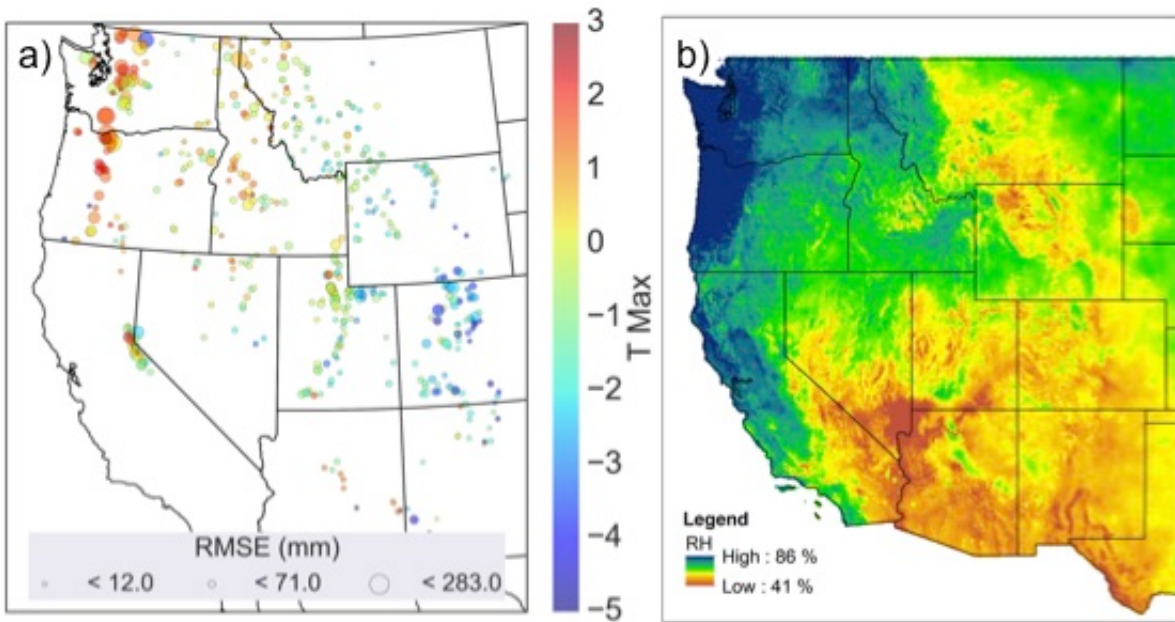
1339

1340 Figure 2: The phase of precipitation at the ground surface is strongly controlled by atmospheric  
 1341 profiles of temperature and humidity. While conditions exist that are relatively easy to predict  
 1342 rain (a) and snow (b), many conditions lead to complex heat exchanges that are difficult to  
 1343 predict with ground based observations alone (c). The blue dotted line represents the mixing  
 1344 ratio.  $H$ ,  $LE$ ,  $f(sat)$ , and  $r$  are abbreviations for sensible heat, latent heat of evaporation, function  
 1345 of saturation and mixing ratio respectively. The arrow after  $H$  or  $LE$  indicate the energy of the  
 1346 hydrometeor either increasing (up) or decreasing (down) which is controlled by other  
 1347 atmospheric conditions.

1348

1349



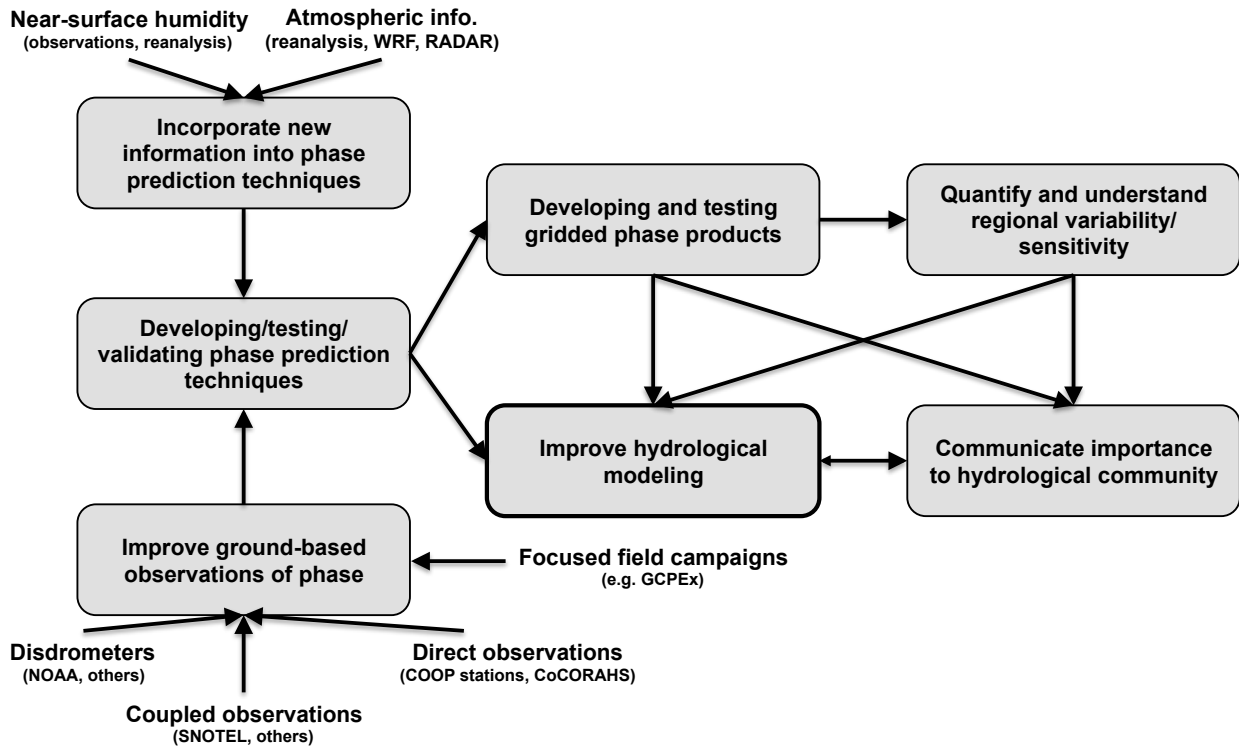


1350

1351 Figure 3: The optimized critical maximum daily temperature threshold that produced the lowest  
 1352 Root Mean Square Error (RMSE) in the prediction of snowfall at Snow Telemetry (SNOTEL)  
 1353 stations across the western US (adapted from Rajagopal and Harpold, 2016). b) Precipitation day  
 1354 relative humidity averaged over 1981-2015 based on the Gridmet dataset (Abatzoglou, 2013).

1355

1356



1357

1358 Figure 4: Conceptual representation of the research gaps and workflows needed to advance PPM  
1359 and improve hydrological modeling.

1360

1361 Table 1. Common hydrological models and the precipitation phase prediction (PPM) technique  
 1362 employed. The citation referring to the original publication of the model is given.

<b>Model</b>	<b>PPM technique</b>	<b>Citations</b>
<u>Discrete Models (not coupled)</u>		
HBV	Static Threshold	Bergström, 1995
Snowmelt Runoff Model	Static Threshold	Martinec et al., 2008
SLURP	Static Threshold	Kite, 1995
UBC Watershed Model	Linear Transition	Pipes and Quick, 1977
PRMS model	Minimum & Maximum Temperature	Leavesley et al., 1996
USGS water budget	Linear transition between two mean temps	McCabe and Wolock, 1999a
SAC-SMA (SNOW-17)	Static Threshold	Anderson, 2006
DHSVM	Linear transition (double check)	Wigmosta et al., 1994
SWAT	Threshold Model	Arnold et al., 2012
RHESSys	Linear transition or input phase	Tague and Band, 2004
HSPF	Air and dew point temperature thresholds	Bicknell et al., 1997
THE ARNO MODEL	Static Threshold	Todini, 1996
HEC-1	Static Threshold	HEC-1, 1998
MIKE SHE	Static Threshold	MIKE-SHE User Manual
SWAP	Static Threshold	Gusev and Nasonova, 1998
BATS	Static Threshold	Yang et al., 1997
Utah Energy Balance	Linear Transition	Tarboton and Luce, 1996
SNOBAL/ISNOBAL	Linear Transition*	Marks et al., 2013
CRHM	Static Threshold	Fang et al., 2013
GEOTOP	Linear Transition	Zanotti et al. 2004
SNTHERM	Linear Transition	SNTHERM Online Documentation
<u>Offline LS models</u>		
Noah	Static Threshold	Mitchell et al., 2005
VIC	Static Threshold	VIC Documentation
CLASS	Multiple Methods <sup>+</sup>	Verseghy, 2009

1363  
 1364 \* by default. Temperature-phase-density relationship explicitly specified by user.

1365 + A flag is specified which switches between, static threshold, linear transition.

1366  
 1367  
 1368  
 1369  
 1370  
 1371  
 1372

1373 Table 2: Remote sensing technologies useful to precipitation phase discrimination organized into  
 1374 ground-based, spaceborne with passive microwave, and passive with active microwave. The  
 1375 table describes the variables of interest, their temporal and spatial coverage, and associated  
 1376 references.

Technology	Variables	Spatial resolution; coverage	Temporal resolution, period of record	References
<b><i>Ground-based systems</i></b>				
Vertically pointing, single polarized 915-MHz Doppler wind profilers	Reflectivity, brightband height, Doppler vertical velocity	100 m vertical resolution; deployed locally in Sierra Nevada basins	Hourly, Winters 1998, 2001 - 2005	White et al., 2002; Lundquist et al., 2008
NEXRAD Dual polarized radar	Reflectivity <sup>1</sup> , hydrometeor classification <sup>1</sup> , melting layer <sup>1</sup> , hybrid hydrometeor classification <sup>1</sup>	0.5° azimuthal by 250 m; range 460 km; Nationwide <sup>2</sup>	5 - 10 minutes; 2011 <sup>3</sup> - present	Giangrande et al., 2008; Park et al., 2009; Elmore, 2011; Grazioli et al., 2015
<b><i>Spaceborne systems: Passive microwave</i></b>				
NOAA-15, NOAA-16, NOAA-17 Advanced Microwave Sounding Unit-A, B	Brightness temperature	48 km (AMSU-A), 16 km (AMSU-B); global coverage, with 22000 km swath	For two platforms, 6 hours revisit time; three platforms, 4 hours revisit time <sup>4</sup> ; 1998 - present	Kongoli et al., 2003
SUOMI-NPP Advanced Technology Microwave Sounder	Brightness temperature	15 - 50 km; global coverage, with 2200 km swath	Daily; 2011 - present	Kongoli et al., 2015
GPM Core Observatory Microwave Imager	Brightness temperature	4.4 km by 7.3 km; global coverage, 904 km swath	2014 to present	Skofronick-Jackson et al., 2015
<b><i>Spaceborne systems: Active microwave</i></b>				
Cloud Profiling Radar (CPR)	Radar reflectivity, 2C-SNOW-PROFILE	1.4 by 1.7 km; swath 1.4 km	16 days; 2006 to present	Wood et al., 2013; Cao et al., 2014; Kulie et al., 2016;
GPM Core Observatory Dual-frequency Precipitation Radar	Radar reflectivity	5 km; global coverage, 120 - 245 km swath	2 - 4 hours; 2014 to present	Skofronick-Jackson et al., 2015

1377 *Notes:*

1378 1. Operational products available from NOAA (2016). The operational products are not ground validated, except  
 1379 where analyzed for specific studies.

1380 2. The dates given here represent the first deployments. Data temporal coverage will vary by station.

1381 3. Gaps in coverage exist, particularly in Western States.

1382 4. Similar instruments mounted on the NASA Aqua satellite and the European EUMETSAT MetOp series. Taking  
 1383 into account the similar instrumentation on multiple platforms increases the temporal spatial resolution